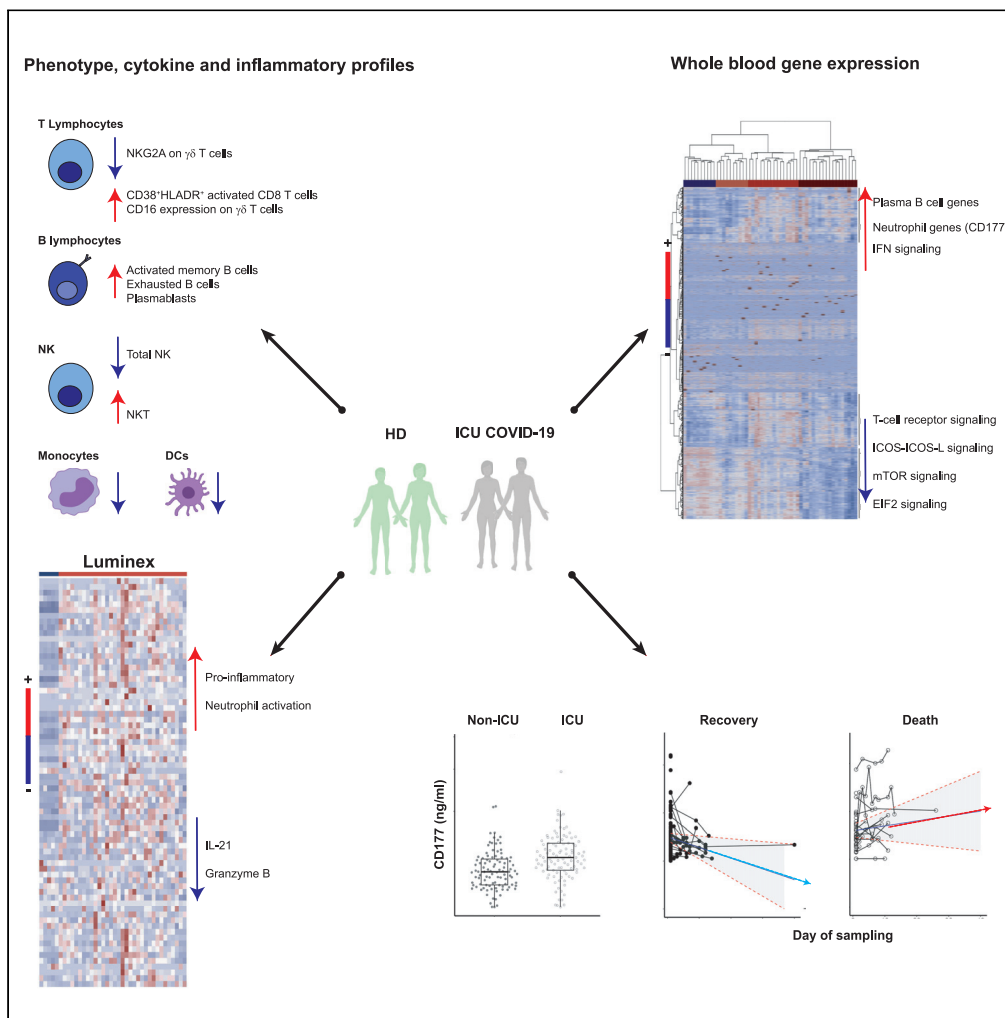


Article

CD177, a specific marker of neutrophil activation, is associated with coronavirus disease 2019 severity and death



Yves Lévy, Aurélie Wiedemann, Boris P. Hejblum, ..., Giuseppe Pantaleo, Hakim Hocini, Rodolphe Thiébaud

yves.levy@aphp.fr (Y.L.)
 rodolphe.thiebaud@u-bordeaux.fr (R.T.)

Highlights

Increase in B cells, activated CD8 T cells, NKT, and $\gamma\delta$ T NKG2A + cells in severe COVID-19

Severe COVID-19 is characterized by an increase of neutrophil and inflammatory markers

Serum CD177 protein levels are increased in patients with COVID-19 in ICU

Sustained high levels of CD177 discriminated recovery and death of patients with COVID-19



Article

CD177, a specific marker of neutrophil activation, is associated with coronavirus disease 2019 severity and death

Yves Lévy,^{1,2,14,*} Aurélie Wiedemann,^{1,11} Boris P. Hejblum,^{1,3,11} Mélyny Durand,^{1,3} Cécile Lefebvre,¹ Mathieu Surénaud,¹ Christine Lacabartz,¹ Matthieu Perreau,⁴ Emile Foucat,¹ Marie Déchenaud,¹ Pascaline Tisserand,¹ Fabiola Blengio,¹ Benjamin Hivert,³ Marine Gauthier,³ Minerva Cervantes-Gonzalez,^{5,6,7} Delphine Bachelet,^{5,7} Cédric Laouéan,^{5,7} Lila Bouadma,⁸ Jean-François Timsit,⁸ Yazdan Yazdanpanah,^{6,7} Giuseppe Pantaleo,^{1,4,9} Hakim Hocini,^{1,12} Rodolphe Thiébaud,^{1,3,10,12,*} and the French COVID cohort study group¹³

SUMMARY

The identification of patients with coronavirus disease 2019 and high risk of severe disease is a challenge in routine care. We performed cell phenotypic, serum, and RNA sequencing gene expression analyses in severe hospitalized patients (n = 61). Relative to healthy donors, results showed abnormalities of 27 cell populations and an elevation of 42 cytokines, neutrophil chemo-attractants, and inflammatory components in patients. Supervised and unsupervised analyses revealed a high abundance of CD177, a specific neutrophil activation marker, contributing to the clustering of severe patients. Gene abundance correlated with high serum levels of CD177 in severe patients. Higher levels were confirmed in a second cohort and in intensive care unit (ICU) than non-ICU patients (P < 0.001). Longitudinal measurements discriminated between patients with the worst prognosis, leading to death, and those who recovered (P = 0.01). These results highlight neutrophil activation as a hallmark of severe disease and CD177 assessment as a reliable prognostic marker for routine care.

INTRODUCTION

The coronavirus disease 2019 (COVID-19) pandemic is caused by a newly described highly pathogenic beta coronavirus, severe acute respiratory syndrome coronavirus 2 (SARS-CoV-2) (Coronaviridae Study Group of the International Committee on Taxonomy of, 2020; Phelan et al., 2020). COVID-19 consists of a spectrum of clinical symptoms that range from mild upper respiratory tract disease in most cases to severe disease that affects approximately 15% of patients requiring hospitalization (Wu and McGoogan, 2020), some of whom require intensive care because of severe lower respiratory tract illness, acute respiratory distress syndrome, and extrapulmonary manifestations, leading to multiorgan failure and death. Several recent studies have provided important clues about the physiopathology of COVID-19 (Blanco-Melo et al., 2020; Chen et al., 2020a; Kuri-Cervantes et al., 2020; Mehta et al., 2020; Qin et al., 2020). Most compared the immune and inflammatory status of patients at different stages of the disease (Hadjadj et al., 2020; Mathew et al., 2020; Wilk et al., 2020). Thus, several important biomarkers associated with specific phases of the evolution of COVID-19 have thus far been identified (Ponti et al., 2020; Silvin et al., 2020). Inflammation, cytokine storms, and other dysregulated immune responses have been shown to be associated with severe disease pathogenesis (Lucas et al., 2020; Ong et al., 2020). Patients with severe COVID-19 are characterized by elevated numbers of monocytes and neutrophils and lymphopenia (Giamarellos-Bourboulis et al., 2020; Huang et al., 2020; Mathew et al., 2020; Zhou et al., 2020), and a high neutrophil-to-lymphocyte ratio predicts in-hospital mortality of critically ill patients (Fu et al., 2020). High levels of proinflammatory cytokines, including interleukin (IL)-6, IL-1 β , tumor necrosis factor (TNF), MCP-1, IP-10, and granulocyte colony-stimulating factor (G-CSF), in the plasma (Chen et al., 2020a, 2020b; Giamarellos-Bourboulis et al., 2020; Mathew et al., 2020; Zhou et al., 2020) and a possible defect in type I interferon (IFN) activity have been reported in patients with severe COVID-19 (Arunachalam et al., 2020; Hadjadj et al., 2020; Ong et al., 2020). However, these responses are dynamic, changing rapidly during the clinical course of the disease, which

¹Vaccine Research Institute, Université Paris-Est Créteil, Faculté de Médecine, INSERM U955, Team 16, Hôpital Henri Mondor, 51 Av Marechal de Lattre de Tassigny, 94010 Créteil, France

²Assistance Publique-Hôpitaux de Paris, Groupe Henri-Mondor Albert-Chenevier, Service Immunologie Clinique, Créteil, France

³Univ. Bordeaux, Department of Public Health, INSERM U1219 Bordeaux Population Health Research Centre, Inria SISTM, UMR 1219, 146 Rue Leo Saignat, 33076 Bordeaux, France

⁴Swiss Vaccine Research Institute, Lausanne University Hospital, University of Lausanne, Lausanne, Switzerland

⁵AP-HP, Hôpital Bichat, Département Épidémiologie Biostatistiques et Recherche Clinique, INSERM, Centre d'Investigation clinique-Epidémiologie Clinique 1425, F-75018 Paris, France

⁶AP-HP, Hôpital Bichat, Service de Maladies Infectieuses et Tropicales, F-75018 Paris, France

⁷Université de Paris, INSERM, IAME UMR 1137, F-75018 Paris, France

⁸APHP- Hôpital Bichat – Médecine Intensive et Réanimation des Maladies Infectieuses, Paris, France

⁹Immunology and Allergy Service, Department of Medicine, Lausanne

Continued



may explain the high variability of the immunological spectrum described (Arunachalam et al., 2020; Bouadma et al., 2020; Lucas et al., 2020). This makes it difficult to deduce a unique profile of the pathophysiology of this infection, which is still undetermined. Furthermore, the high amplitude of the signals generated by the inflammation associated with the disease may hide other pathways that are involved.

From a clinical standpoint, clinicians face the daily challenge of predicting worsening patients owing to the peculiar clinical course of severe COVID-19, characterized by a sudden deterioration of the clinical condition 7 to 8 days after the onset of symptoms. Determination of the onset of the pathological process once infection has been established in a patient with a severe stage of infection is highly imprecise because of the possible paucisymptomatic or asymptomatic phase of the infection, as well as the low specificity of self-limited “flu” illness.

We used a systems immunology approach to identify host factors that were significantly associated with the time to illness onset, severity of the disease (intensive care unit [ICU] or transfer to ICU), and mortality of patients with COVID-19 enrolled in the multicentric French COVID cohort (Yazdanpanah, 2020). In addition to the depletion of T cells and mobilization of B cells, neutrophil activation, and severe inflammation, we show upregulation of CD177 gene expression and protein levels in the blood of patients with COVID-19 in both the COVID-19 cohort and a “confirmatory” cohort, that is, Swiss cohort, relative to healthy subjects. CD177, a neutrophil activation marker, characterized critically ill patients and marked disease progression and death. Our finding highlights the major role of neutrophil activation through CD177 overexpression in the critical clinical transition point in the trajectory of patients with COVID-19.

RESULTS

Overview of the phenotype, cytokine, and inflammatory profiles of patients with COVID-19

Patient characteristics from the French COVID cohort enrolled in this analysis are shown in Table 1. All patients from this cohort were stratified as severe as per criteria of the French COVID cohort (clinicaltrials.gov NCT04262921) (Yazdanpanah, 2020), with 53 (87%) being hospitalized in an ICU (either initially or after clinical worsening or death) and eight were not. The median age was 60 years (interquartile range, 50–69) and 80% were men. Sampling for immunological analyses was performed within three days of entry and after a median of 11 days [7–14] after the onset of symptoms. We first assessed leukocyte profiles by flow cytometry using frozen peripheral blood mononuclear cells (PBMCs) from 50 patients with COVID-19 (with available PBMC samples) and 18 healthy donors (HDs) (14 or 15 HDs were used as controls per immune cell subset).

We analyzed 52 immune cell populations (gating strategies are shown in Figure S1); of which, 23 showed significant differences (Wilcoxon test adjusted for multiple comparisons) between patients with COVID-19 and HDs. We not only confirmed previously reported abnormalities but also revealed new immunological features of patients with COVID-19 (Figure S2). Patients with COVID-19 showed a significant reduction in the frequency of total CD3⁺ T cells and CD8⁺ T cells relative to HDs, as previously reported (De Biasi et al., 2020; Xu et al., 2020), that expressed an activated phenotype (CD38⁺HLA-DR⁺) (Figure 1A). Patients with COVID-19 also showed lower frequencies of resting memory B cells contrasting with higher frequencies of activated memory B cells and exhausted B cells (Figure 1B). As previously reported (Bouadma et al., 2020; Mathew et al., 2020), the proportion of plasmablasts was markedly higher in patients with COVID-19 (median [Q1–Q3]: 10.85% [3–23]) than HDs (0.76% [0.4–0.8]) (P < 0.001). Total natural killer (NK) cell frequencies, more precisely those of the CD56^{bright} and CD56^{dim}CD57⁻ NK cell subpopulations, were lower than in HDs (P = 0.017, P < 0.001, and P = 0.004, respectively) (Figure 1C), whereas a higher proportion of these NK cells, as well as NKT cells, were cycling, expressing Ki67 antigen (CD56^{bright}: 22% [13–30], CD56^{dim}CD57⁻: 16.8% [11.5–27], and NKT: 10% [5.6–18.2]) (P = 0.003, P = 0.004, and P = 0.001 compared with HD) (Figure 1C). In addition, patients with COVID-19 showed significantly smaller classical (CD14⁺CD16⁻), intermediate (CD14⁺CD16⁺), and nonclassical (CD14⁻CD16⁺) monocyte subpopulations than HDs (P = 0.013, P = 0.017, P < 0.001, respectively) (Figure 1D). Interestingly, patients with COVID-19 tended to exhibit a higher frequency of $\gamma\delta$ T cells than HDs (median 10.4% [7.5–16.1] vs 7.3% [6–10] in HDs; P = 0.068) (Figure 1E), with a significant proportion of $\gamma\delta$ T cells showing higher expression of the activation marker CD16 (P = 0.01) and lower expression of the inhibitory receptor NKG2A (P < 0.001) than HDs (Figure 1E). Finally, we observed markedly smaller frequencies of dendritic cells (DCs) for all populations studied (pre-DC, plasmacytoid DC (pDC), and conventional DC (cDC1 and cDC2) in patients with COVID-19 than in HDs (P < 0.001, for all comparisons) (Figure 1F). Neutrophils count were available in 44 patients, and the concentration was more elevated in patients with COVID-19 belonging to group 2 and group 3 compared with group 1 (8.109/L vs 3.109/L, p < 0.03). It was also more elevated in patients hospitalized in an ICU (8.109/L vs 2.109/L, p < 0.009).

University Hospital, University of Lausanne, Lausanne, Switzerland

¹⁰CHU de Bordeaux, Pôle de Santé Publique, Service d'Information Médicale, Bordeaux, France

¹¹These authors contributed equally

¹²Senior authors

¹³Members of the French COVID study group are listed in Supplementary Information

¹⁴Lead contact

*Correspondence: yves.levy@aphp.fr (Y.L.), rodolphe.thiebaut@u-bordeaux.fr (R.T.)

<https://doi.org/10.1016/j.isci.2021.102711>

Table 1. Patient characteristics of the French COVID cohort (n=61)

	Number of patients	
Demographic characteristics		
Age – median (IQR) – years	61	60 (50–69)
Male sex – No./total No. (%)	61	49/61 (80)
ICU or transfer to ICU or death – No./total No. (%)	61	53/61 (87)
Outcome – No./total No. (%)	61	
Death		21/61 (34)
Discharge alive		40/61 (66)
Median interval from first symptoms on admission (IQR) – days	61	11 (7–14)
Comorbidities – No./total No. (%)		
Any	61	14/61 (23)
Chronic cardiac disease	61	9/61 (15)
Hypertension	61	22/61 (36)
Chronic pulmonary disease	61	5/61 (8)
Asthma	61	4/61 (7)
Chronic kidney disease	61	6/61 (10)
Chronic neurological disorder	61	2/61 (3)
Obesity	60	23/60 (38)
Diabetes	61	12/61 (20)
Smoking History – No./total No. (%)		
Smoking	61	5/61 (8)
Laboratory findings on admission - Median (IQR)		
Hemoglobin – g/dL	57	13 (11–14)
WBC count – $\times 10^9/L$	57	6 (5–9)
Platelet count – $\times 10^9/L$	57	189 (143–270)
C-reactive protein (CRP) – mg/L	57	120 (66–195)
Blood urea nitrogen (urea) – mmol/L	57	7 (5 – 12)
Symptoms on admission – No./total No. (%)		
Fever	59	51/59 (86)
Cough	57	40/57 (70)
Sore throat	56	4/56 (7)
Wheezing	54	6/54 (11)
Myalgia	56	21/56 (38)
Arthralgia	55	9/55 (16)
Fatigue	57	27/57 (47)
Dyspnea	57	46/57 (81)
Headache	57	11/57 (19)
Altered consciousness	56	3/56 (5)
Abdominal pain	53	8/53 (15)
Vomiting/nausea	56	10/56 (18)
Diarrhea	56	11/56 (20)
Clinical characteristics on admission – Median (IQR)		
SOFA score (ICU patients)	34	6 (4–8)

(Continued on next page)

Table 1. Continued

	Number of patients	
SAPS2 (ICU patients)	36	32 (27–53)
Heart rate – beats per minute	61	87 (76–104)
Respiratory rate – breaths per minute	55	24 (20–32)
Systolic blood pressure - mmHg	60	130 (109–145)
Diastolic blood pressure – mmHg	60	77 (70–87)
Oxygen saturation – percent	61	96 (91–98)
Oxygen saturation on – No./total No. (%)	56	
Room air		17/56 (30)
Oxygen therapy		39/56 (70)
Treatments – No./total No. (%)		
Antiviral	60	40/60 (66)
Antibiotic	60	46/60 (77)
Corticosteroids	60	33/60 (55)
Antifungal	60	9/60 (15)
Hydroxychloroquine	59	8/59 (14)

We then evaluated the levels of 71 serum cytokines, chemokines, and inflammatory factors in 33 patients with COVID-19 and 5 HDs. Forty-four analytes differed significantly (Wilcoxon test adjusted for multiple comparisons) between the patients with COVID-19 and HDs (shown in the heatmap in [Figure 2](#) and detailed in [Figure S3](#)). The levels of 42 factors were higher, among them, proinflammatory factors (IL-1a, IL-6, IL-18, TNF alpha and β [TNF- α , TNF- β], IL-1ra, ST2/IL-1R4, the acute phase protein lipopolysaccharide-binding protein LBP, IFN- α 2); Th1 pathway factors (IL-12 [p70], IFN- γ , IP-10, IL-2Ra); Th2/regulatory cytokines (IL-4, IL-10, IL-13); IL-17, which also promotes G-CSF-mediated granulopoiesis and recruits neutrophils to inflammatory sites; T cell proliferation and activation factors (IL-7, IL-15); growth factors (SCF, SCGF-b, HGF, b-FGF, b-NGF); and a significant number of cytokines and chemokines involved in macrophage and neutrophil activation and chemotaxis (RANTES (CCL5), MIP-1a and b (CCL3 and CCL4), MCP-1 (CCL2), MCP-3 (CCL7), M-CSF, MIF, Gro-a (CXCL1), monokine inducible by γ IFN MIG/CXCL9, IL-8, IL-9). Interestingly, we found higher levels of midkine, a marker usually not detectable in the serum, which enhances the recruitment and migration of inflammatory cells and contributes to tissue damage ([Cai et al., 2020](#)). In parallel, granzyme B and IL-21 levels were significantly lower in patients with COVID-19 patients than HDs ($P = 0.007$ and $P = 0.004$, respectively) ([Figure S3](#)).

Whole blood gene expression profiles show a specific signature for patients with COVID-19

The comparison of gene abundance in whole blood between patients with COVID-19 ($n = 44$) and HDs ($n = 10$) showed 4,079 differentially expressed genes (DEGs) with an absolute fold change ≥ 1.5 , including 1,904 that were upregulated and 2,175 that were downregulated ([Figure 3A](#)). The main pathways associated with the DEG correspond to the immune response, including neutrophil and IFN signaling, T and B cell receptor responses, metabolism, protein synthesis, and regulators of the eIF2 and mammalian target of rapamycin (mTOR) signaling pathways ([Figure 3A](#)). Although several of these pathways involved multiple cell types, analysis of the neutrophil pathway showed higher abundance of genes mainly related to neutrophil activation, their interaction with endothelial cells, and migration ([Figure 3B](#)). Among the most highly expressed genes, this signature included *CD177*, a specific marker of neutrophil adhesion to the endothelium and transmigration ([Bayat et al., 2010](#)), *HP* (haptoglobin), a marker of granulocyte differentiation and released by neutrophils in response to activation ([Theilgaard-Monch, 2006](#)), *VNN1* (hematopoietic cell trafficking), *GPR84* (neutrophil chemotaxis), *MMP9* (neutrophil activation and migration), and *S100A8* and *S100A12* (neutrophil recruitment, chemotaxis, and migration). The *S100A12* protein is produced predominantly by neutrophils and is involved in inflammation and the upregulation of vascular endothelial cell adhesion molecules ([Roth et al., 2003](#)) ([Figure 3B](#)).

In parallel, we observed a higher abundance of several IFN-stimulating genes (ISGs) (*IFI27*, *IFITM3*, *IFITM1*, *IFITM2*, *IFI6*, *IRF7*, *IRF4*) ([Figure 3C](#)) and cytokines and cytokine receptors (*IL-1R*, *IL-18R1*, *IL-18RAP*, *IL-4R*, *IL-17R*, *IL-10*) ([Figure 3D](#)). Consistent with profound T cell lymphopenia, the expression of several families of

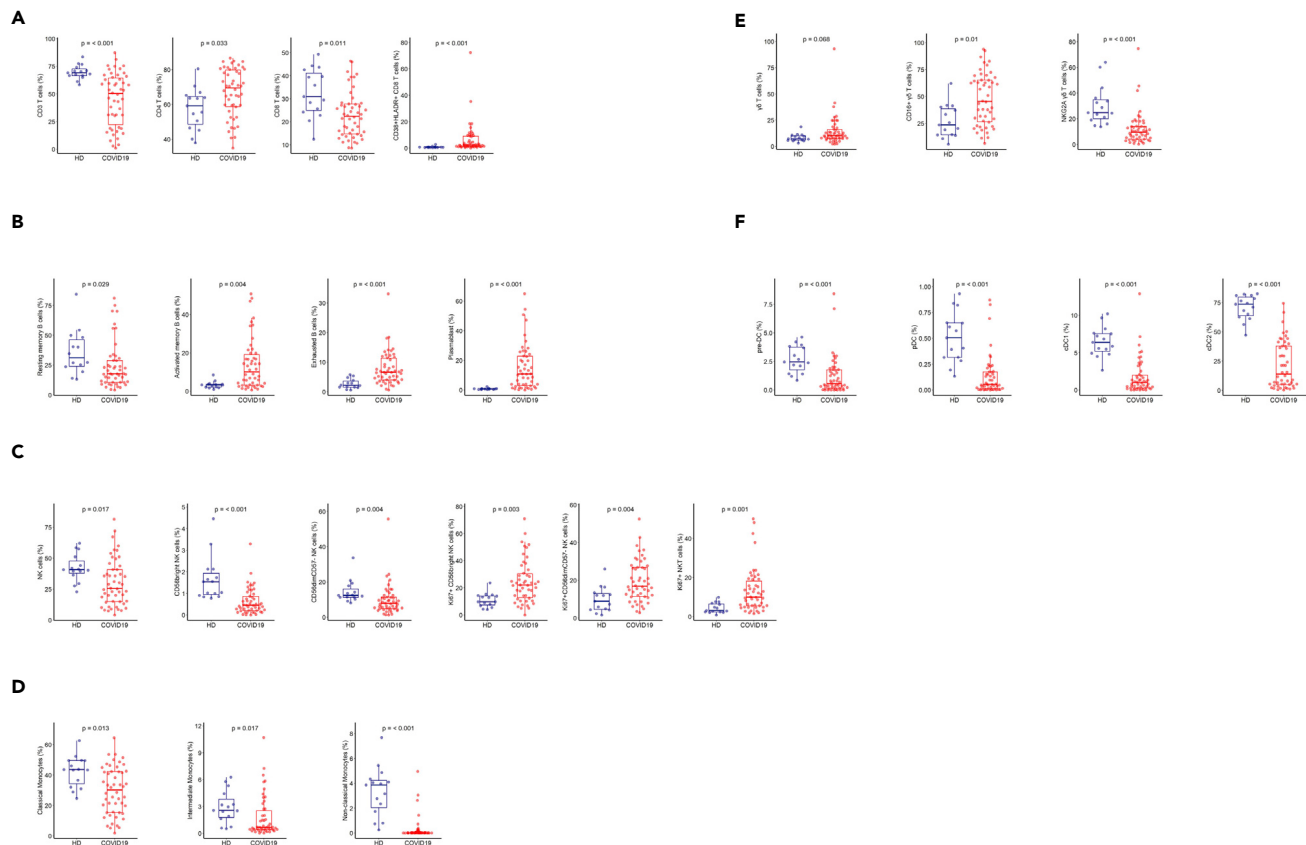


Figure 1. Frequency of immune-cell subsets between HDs (n = 18) and patients with COVID-19 (n = 50)

(A) Frequency of total CD3 T cells, CD4 and CD8 T cell subsets, and activated CD38⁺HLADR⁺ CD8 T cells.

(B) Frequency of B cell subsets (CD21⁺CD27⁺: resting memory, CD21⁻CD27⁺: activated memory, CD21⁻CD27⁻: exhausted) and plasmablasts (CD38⁺+CD27⁺) gated on CD19⁺ B cells.

(C) Frequency of NK cell subsets (gated on CD3⁻CD14⁻CD56^{Bright}: CD56⁺⁺CD16⁺, CD56^{dim}: CD56⁺CD16⁺⁺CD57^{+/-}, differentiated Ki67⁺ NK cells (gated on CD56^{Bright} or CD56^{dim}CD57⁻ NK cells) and differentiated Ki67⁺ NKT cells (gated on CD3⁺CD56⁺ cells).

(D) Monocyte subsets (gated on CD3⁻CD56⁻) (classical monocytes: CD14⁺CD16⁻, intermediate monocytes: CD16⁺CD14⁺, non-classical monocytes: CD14⁻CD16⁺).

(E) Frequency of $\gamma\delta$ T cells (gated on CD3⁺ T cells) and CD16 and NKG2A expression (gated on $\gamma\delta$ CD3⁺ T cells).

(F) Frequency of DC subsets (gated on HLADR⁺Lin⁻) (pDC: CD45RA⁺CD33⁻CD123⁺, pre-DC: CD123⁺CD45RA⁻, cDC1: CD33⁺CD123⁻CD141⁺CD1c^{low}, cDC2: CD33⁺CD123⁻CD14⁺CD1c⁺) detected by flow cytometry in PBMCs from n = 50 patients with COVID-19 and n = 18 HDs. The differences between the two groups were evaluated using Wilcoxon rank sum statistical tests. The lower and upper boundaries of the box represent the 25% and 75% percentiles, the whiskers extend to the most extreme data point that is no more than 1.5 times the interquartile range away from the box. Median values (horizontal line in the boxplot) are shown.

See also [Figures S1](#) and [S2](#).

T cell receptor genes was lower ([Figure 3E](#)). We observed severe dysregulation of T cell function that involved inhibition of serine/threonine kinase PKC θ signaling (Z score = -4.46), as well as the inducible T cell costimulator/ICOSL axis (Z score = -4.5) ([Figure S4](#)). In contrast to the results for T cells, the peripheral expansion of memory B cells and plasmablasts was associated with broad expansion of the B cell receptor (BCR) ([Figure 3F](#) and [Table S2](#)).

We also observed genes belonging to several crucial pathways and biological processes that had not been previously reported to characterize patients with COVID-19 to be underrepresented. These included eIF2 signaling, with many downregulated genes, such as ribosomal proteins and eukaryotic translation initiation factors ([Figure S4A](#)), common targets of the integrated stress response (ISR), including antiviral defense ([Levin and London, 1978](#); [Pakos-Zebrucka et al., 2016](#)). In addition, we also found genes involved in signaling through mTOR ([Figure S4B](#)), a member of the phosphatidylinositol-3-kinase-related kinase family

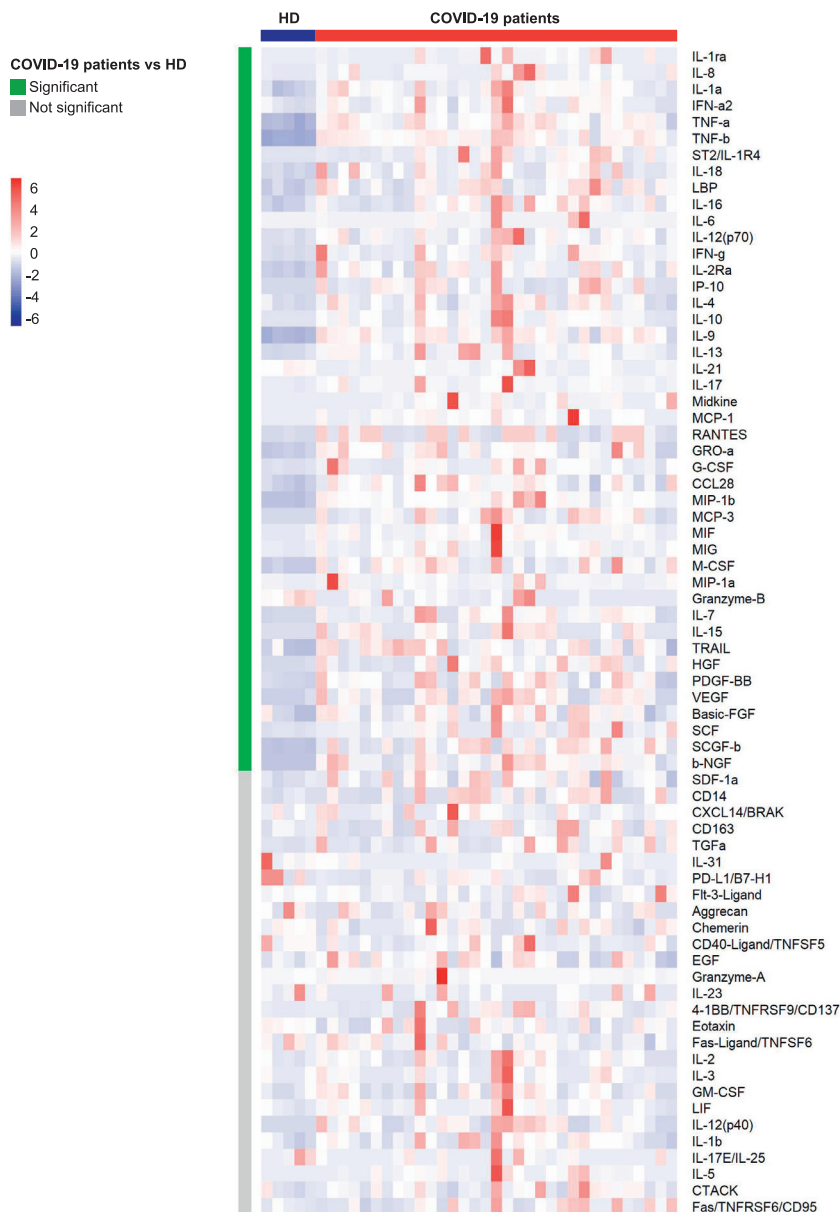


Figure 2. Heatmap of analyte abundance in serum

The colors represent standardized expression values centered around the mean, with variance equal to 1. HD: healthy donors (n = 5), COVID: patients with COVID-19 (n = 33). Each column represents a subject. Each line represents an analyte. See also [Figure S3](#).

of protein kinases. Prediction analysis using Ingenuity pathways showed both lower eIF2 (Z score = - 6.8) and mTOR (Z score = -2.2) signaling in patients with COVID-19 than HDs.

Unsupervised whole blood gene expression profiles reveal distinct features of patients with COVID-19

Unsupervised classification of 44 patients with COVID-19 and 10 HDs identified three distinct groups of patients with COVID-19: 10 in group 1, 16 in group 2, and 18 in group 3 ([Figure 4](#)). Detailed patient characteristics as per the group are presented in [Table S1](#). Among a large set of clinical and biological characteristics, the analysis showed the differential clustering to not be explained by the severity of the disease. Indeed, the median Sequential Organ Failure Assessment (SOFA) score and Simplified Acute Physiology

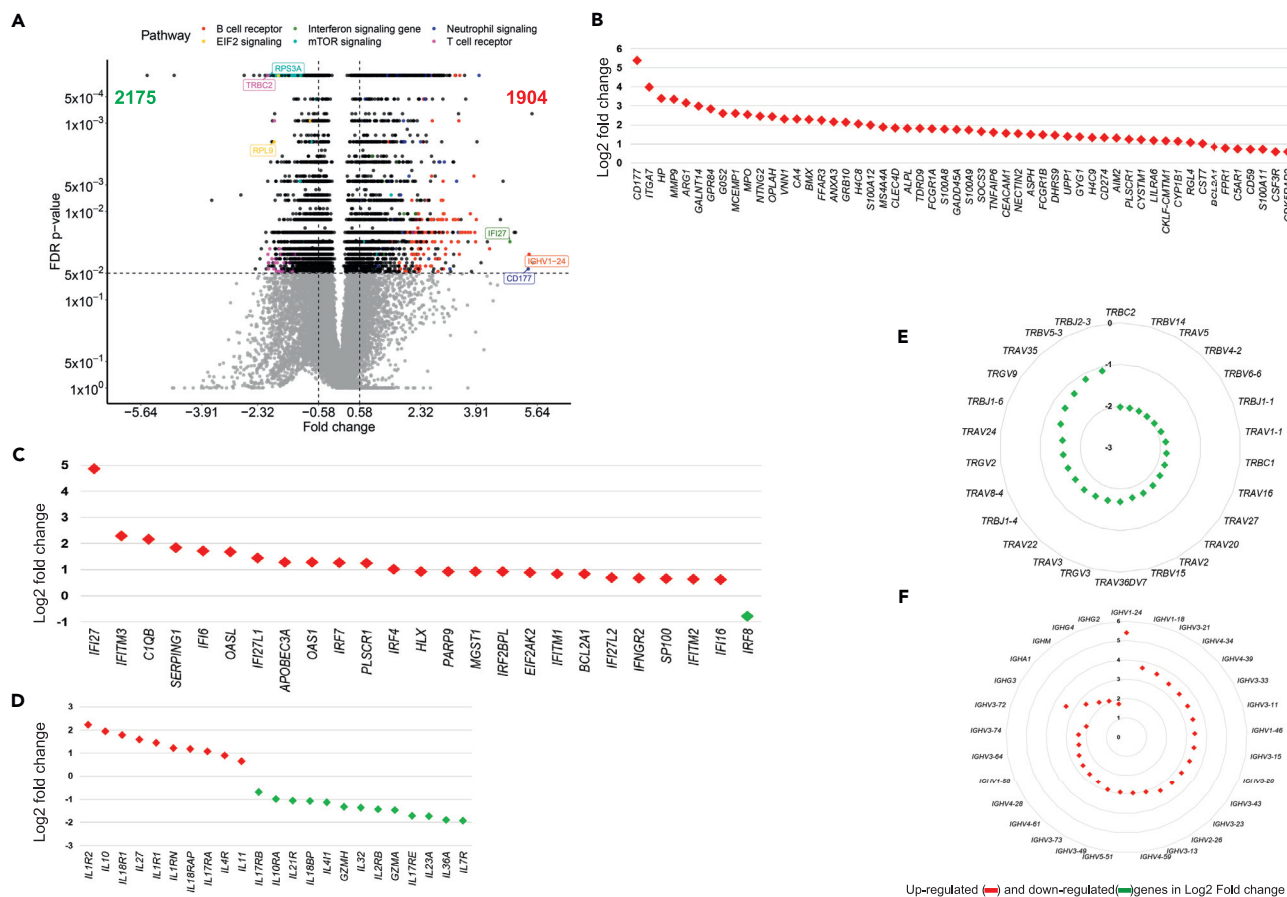


Figure 3. Whole blood gene expression in COVID-19 patients and HDs

(A) Volcano plot showing differentially expressed genes (DEG) as per the log₂ fold change (log₂ FC) and Benjamini-Hocberg False Discovery Rate (FDR) with thresholds at absolute log₂ FC ≥ log₂(1.5) and FDR ≤ 0.05.

(B) Main top DEG related to neutrophils.

(C and D) Main DEG related to IFN and interleukin responses, respectively.

(E) Main TCRV T cell repertoire DEG.

(F) Main B-cell IGHV repertoire DEG. Red symbols represent overabundant genes in COVID-19 relative to HD, green symbols represent underabundant genes.

See also [Figure S4](#) and [Table S2](#).

Score (SAPS2), which include a large number of physiological variables (Le Gall, 1993; Vincent et al., 1998) and evaluate the clinical severity of the disease (a high score is associated with a worse prognosis) of patients with COVID-19, were 6 [4–7] and 36 [28–53], respectively, with no significant differences between groups. Nevertheless, we observed a significant difference from symptoms onset to the admission, which ranged from 7 [6–11] days for patients in group 1 to 11 [10–14] and 13 [9–14] days for patients in groups 2 and 3, respectively (P = 0.04, Kruskal-Wallis test). Finally, group 1 which was the closest to HDs in terms of gene profile consisted of patients in the early days of the disease (Table S1).

Analysis of the genes contributing to the differences between groups confirmed and extended the findings described previously (Figures 3 and S4). Several pathways were highly represented in sectors of the heatmap defined as per gene abundance across patient groups. For example, 97% of the genes making up the BCR and 65% of those involved in neutrophil responses were represented among the genes showing a greater abundance in COVID-19 groups 2 and 3 than group 1 and HDs (Figure 4). Other pathways, such as those for IFN (64%), TCR (100%), iCOS-iCOS-L (88%), mTOR (81%), and eIF2 signaling (92%) were also highly represented. The IFN-signaling genes, such as *IFI44L*, *IFIT2*, and *IRF8*, a regulator of type I IFN (α , β), were significantly more abundant at earlier stages (in patients from group 2) and tended to be less abundant in group 3, at more advanced stages of the disease. Finally, the abundance of genes belonging to

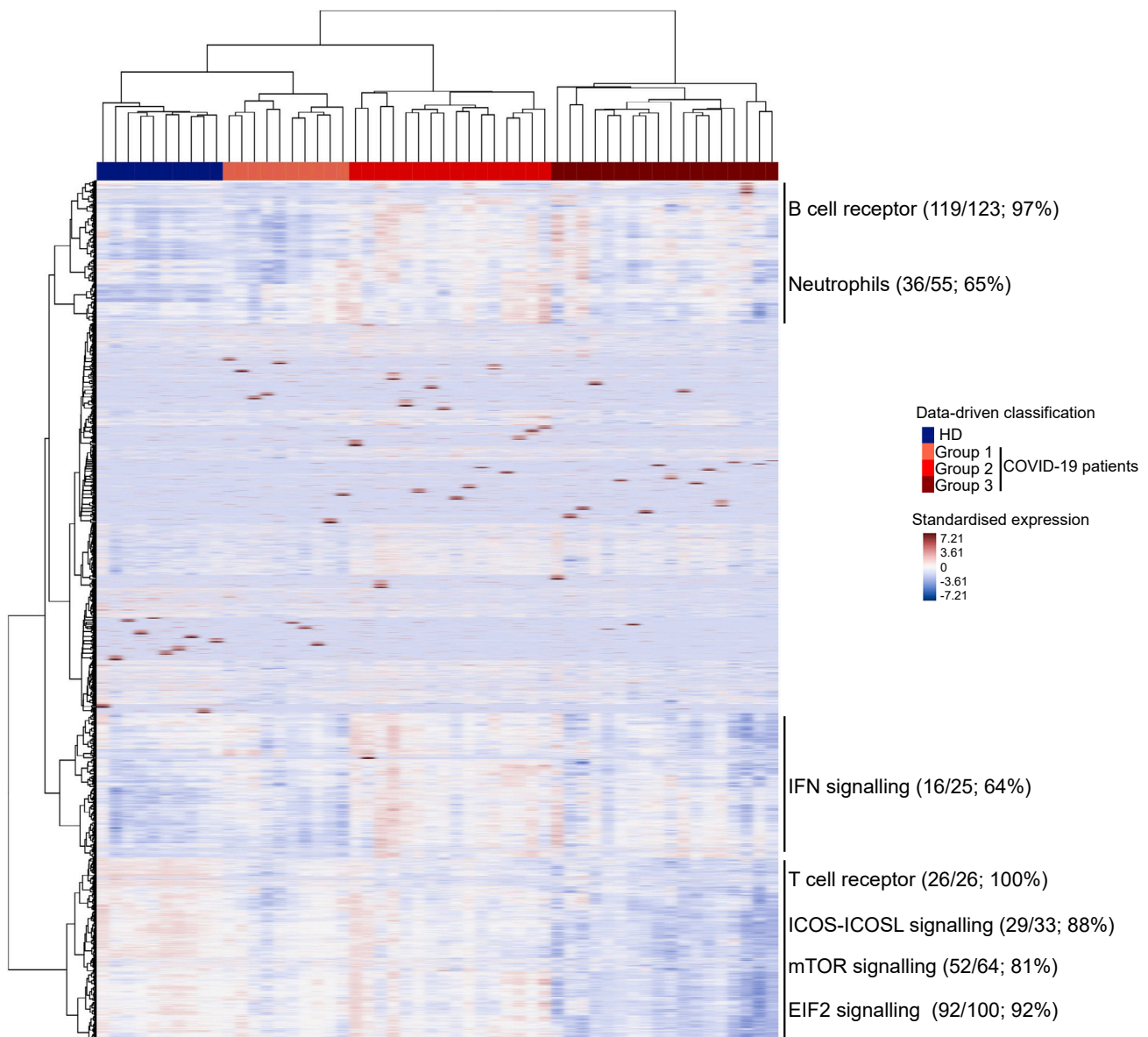


Figure 4. Heatmap of standardized gene expression

The colors represent standardized expression values centered around 0, with variance equal to 1. Each column represents a subject. This heatmap was built by unsupervised hierarchical clustering of log₂-counts-per-million RNA-seq transcriptomic data from whole blood (29,302 genes) and subjects (n = 54) using the Euclidean distance and Ward's method. Seven blocks are highlighted as per the features of gene expression across the groups of individuals. Enrichment (number and % of genes of a given pathway selected in the block) of pathways of interest are shown for each block. See also [Table S1](#).

T cell pathways (TCR, iCOS-iCOSL signaling) or mTOR and eIF2 signaling was lower in group 3, that is to say, those who were analyzed after a longer time from symptom onset to the admission. The findings described previously highlight the heterogeneity of patients with COVID-19.

Integrative analysis of all biomarkers reveals the major contribution of CD177 in the clinical outcome of patients with COVID-19

We performed an integrative analysis using all available data to disentangle the relative contribution of the various markers at the scale of every patient. We thus pooled the data for 29,302 genes from whole blood RNA sequencing (RNA-seq), cell phenotypes (52 types), and cytokines (71 analytes) using the recently

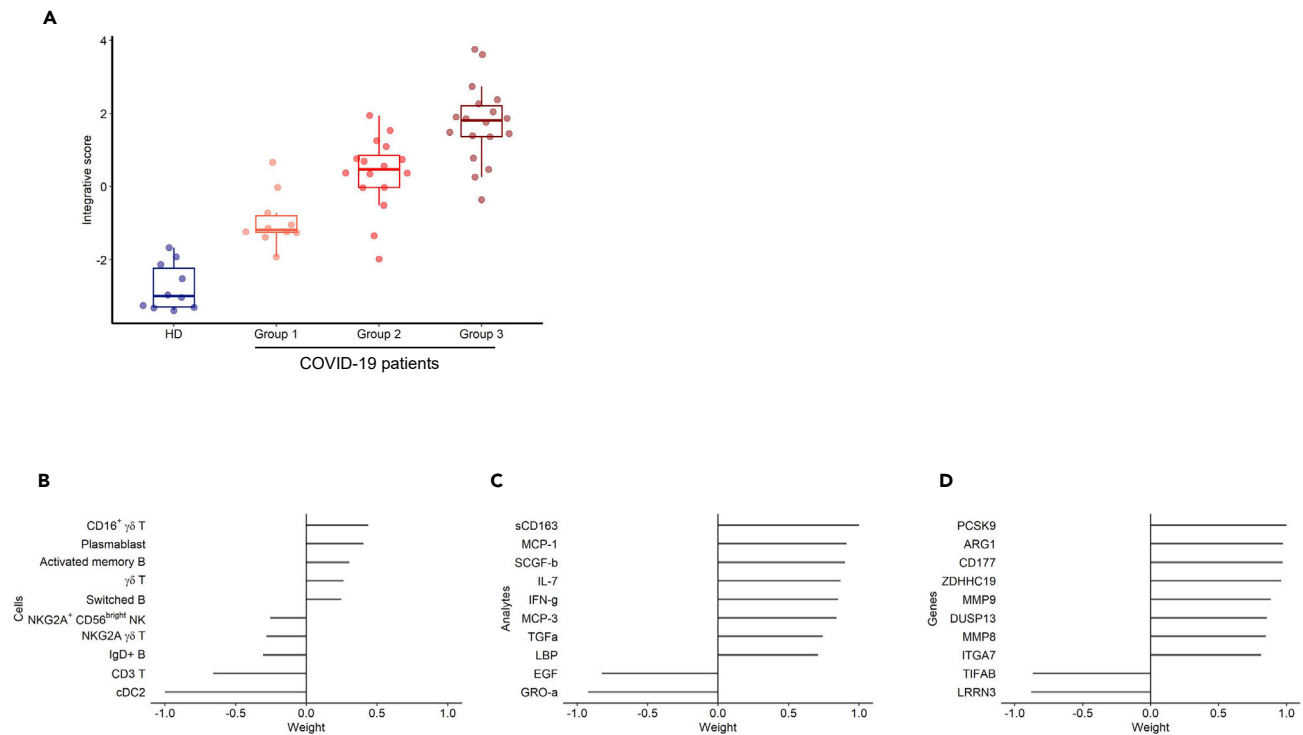


Figure 5. Integrative analysis. Integrative analysis of the data of RNA-seq (29,302 genes) from 44 patients with COVID-19, cell phenotype (52 types) from 45 patients with COVID-19, and serum analytes (71 analytes) from 33 patients with COVID-19 using a sparse principal component analysis approach, MOFA v2

(A–D)(A) Integrative score as per the patient groups defined by the hierarchical clustering of the RNA-seq data. Top 10 marker contributions (as per the weight from -1 to 1) of the cell phenotypes (B), serum analytes (C), and RNA-seq (D). The integrative score corresponds to the first factor of the analysis and allows the ordering of individuals along an axis centered at 0. Individuals with an opposite sign for the factor therefore have opposite characteristics. See also [Figure S5](#).

described MOFA approach ([Argelaguet et al., 2019](#)), which is a statistical framework for dimension reduction adapted to the multiomics context. The data are reduced to components that are linear combinations of variables explaining interpatient variability across the three biological measurement modalities. The first component, that we called our integrative score, discriminated between the three groups of RNA sequencing (initially defined by hierarchical classification based on gene abundance only) and HDs ([Figure 5A](#)), although it only explained a portion of the variability within each of the three types of markers (14% of gene expression, 14% of cell phenotypes, and 5% of cytokines). [Figures 5B–5D](#) show the contribution of each type of markers to the integrative score. The main contributors for the cell phenotype were the significantly lower frequency of cDC2 and T cells and, marginally, the higher number of plasmablasts and CD16⁺ γδ T cells in patients with COVID-19 ([Figure 5B](#)). The contribution of soluble factors was marked by higher levels of soluble CD163 (sCD163), a marker of polarized M2 macrophages involved in tissue repair ([Zhi et al., 2017](#)), in more advanced COVID-19 groups ([Figure 5C](#)). Indeed, CD163 gene expression was also significantly higher in patients with COVID-19 than in HDs (\log_2 fold change = $+1.55$; $FDR = 4.79 \times 10^{-2}$). sCD163 has also been reported to be a marker of disease severity in critically ill patients with various inflammatory or infectious conditions ([Buechler et al., 2013](#)). Interestingly, the genes that contribute the most to the synthesis of this factor were part of the neutrophil module (CD177, ARG1, MMP9) ([Figure 5D](#)). Integrated analysis also revealed higher expression of proprotein convertase subtilisin/kexin type 9 (PCSK9). High plasma PCSK9 protein levels highly correlate with the development and aggravation of subsequent multiple organ failure during sepsis ([Boyd et al., 2016](#); [Dwivedi et al., 2016](#)). Of note, high PCSK9 levels have been recently associated with severe Dengue infection ([Gan et al., 2020](#)). Finally, the increasing abundance of CD177 gene expression as per the group was again clearly apparent ([Figure S4](#)). An additional cell-type-specific significance analysis has been performed to check the robustness of the CD177 differential expression according to the cell-type frequencies ([Shen-Orr et al., 2010](#)). We found that CD177 differential expression between patients with COVID-19 and HD was not fully explained by population variations. Indeed,

Table 2. Characteristics of patients involved in the CD177 analysis

	Number of patients	French cohort (n = 115)	Swiss cohort (n = 88)
Demographic characteristics			
Age – median (IQR) – years	200	62 (54–72)	63 (57–74)
Male sex – No./total No. (%)	201	82/113 (73)	56/88 (64)
ICU or transfer to ICU or death – No. /total No. (%)	200	61/112 (54)	40/88 (45)
Outcome - No. /total No. (%)			
Death		32/107 (30)	8/66 (12)
Discharge alive		75/107 (70)	58/66 (88)
Median interval from first symptoms on admission (IQT)	192	13 (9-18)	12 (9-17)
Comorbidities - No./total No. (%)			
Chronic cardiac disease	197	22/109 (20)	25/88 (28)
Chronic pulmonary disease	197	14/109 (13)	9/88 (10)
Diabetes	197	23/109 (21)	26/88 (30)
Laboratory findings on admission – Median (IQR)			
C-reactive protein (CRP) – mg/L	34	122 (62–196)	
Lactate dehydrogenase (LDH) UI/L	31	466 (337–533)	
Clinical characteristics on admission – Median (IQR)			
Score SOFA	41	4 (2–7)	
Score SAPS2	40	32 (27–49)	

it remained significant after deconvolution in several leukocytes subpopulations (notably FDR of 0.04 within T cells and 0.03 within monocytes).

Serum CD177 protein levels are associated with the clinical outcome of patients with COVID-19

Given the contribution of the neutrophil activation pathway in the clustering of patients with COVID-19, we sought neutrophil-activation features that could act as possible reliable markers of disease evolution. We focused on CD177 because i) it is a neutrophil-specific marker representative of neutrophil activation, ii) it was the most highly differentially expressed gene in patients, and iii) the protein can be measured in the serum, making its use as a marker clinically applicable. Thus, we used an enzyme-linked immunosorbent assay (ELISA) to quantify CD177 in the serum of 203 patients with COVID-19 (115 patients from the French cohort and 88 patients from the Swiss COVID-19 cohort that we used as “a confirmatory” cohort, patient characteristics are described in Table 2), 21% of whom the measurements were repeated (from 2 to 10 measurements per individual). First, we confirmed the significantly higher median serum protein level in the global cohort of patients with COVID-19 (4.5 [2.2–7.4]) relative to that of 16 HDs (2.2 [0.9–4.2]) ($P = 0.015$, Wilcoxon test) (Figure 6A). Second, we found a robust agreement between CD177 gene expression measured by RNA-seq and CD177 protein levels measured by ELISA (intraclass correlation coefficient 0.88) (Figure 6B).

Then, we examined the association of clinical characteristics and outcomes with serum CD177 concentration at the time of admission. The serum CD177 concentration was positively associated with the time from symptom onset to the admission ($r = 0.22$, $P = 0.0026$) (Figure 6C) and was higher for patients hospitalized in an ICU (6.0 ng/mL [3.5–9.4] vs 3.3 ng/mL [1.5–5.6], $P < 0.001$) (Figure 6D). The association between serum CD177 levels and hospitalization in an ICU was independent of the usual risk factors, such as age, sex, chronic cardiac or pulmonary diseases, or diabetes (multivariable logistic regression, adjusted odds ratio 1.14 per unit increase, $P < 0.001$). We observed a trend toward a positive association with the SOFA and SAPS2 risk scores that was not statistically significant ($P = 0.17$ and $P = 0.074$, respectively) (Figures S6A and S6B). CD177 levels were not associated with other conditions that contribute to a high risk of severe disease, such as diabetes ($P = 0.632$), chronic cardiac disease ($P = 0.833$), chronic pulmonary disease ($P = 0.478$), or age of the patient ($P = 0.83$).

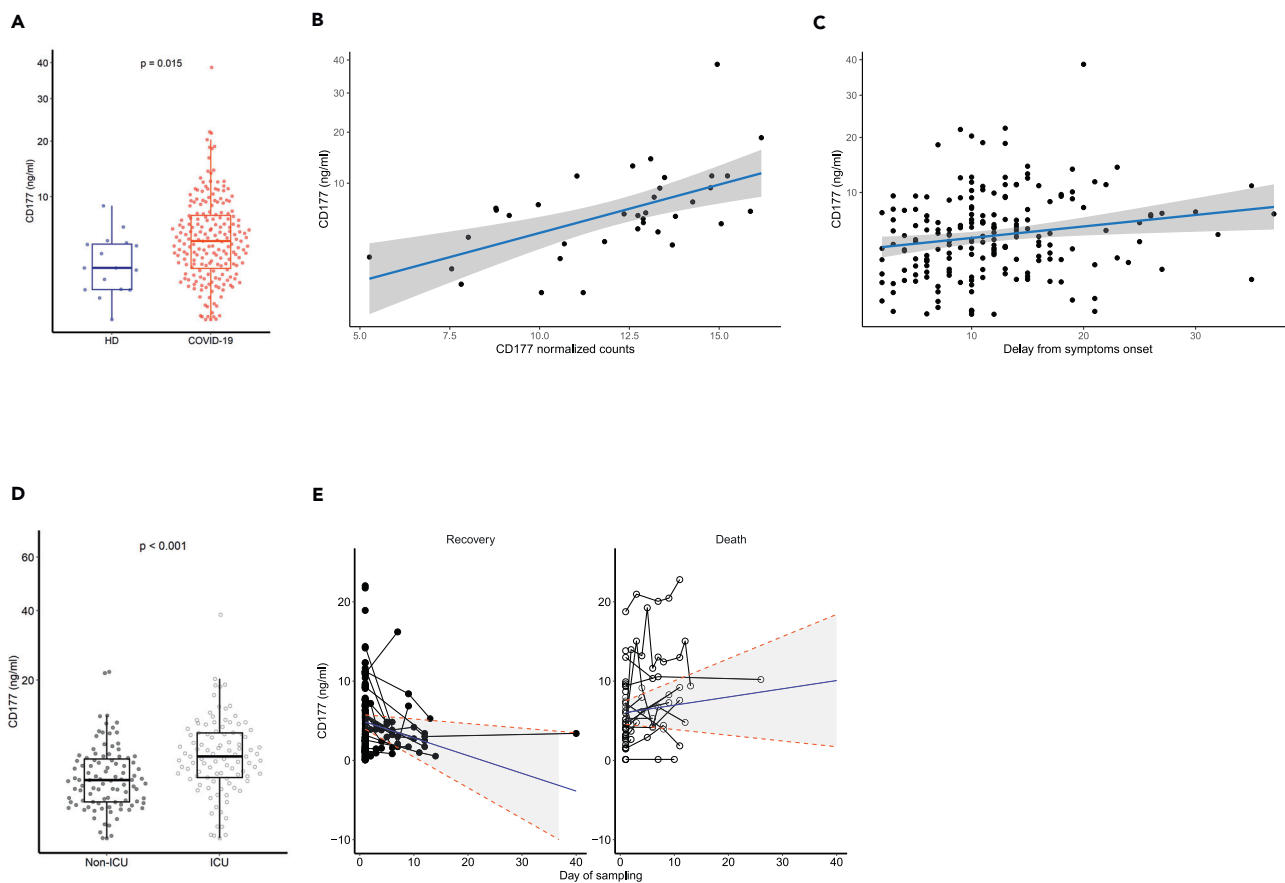


Figure 6. Distribution of the CD177 marker and association with clinical outcomes of patients with COVID-19

(A) Measurement of CD177 (ng/mL). HD: Healthy donors ($n = 16$), patients with COVID-19 ($n = 203$). The difference between the two groups was evaluated using Wilcoxon rank sum statistical tests. The median values (horizontal line in the boxplot) are shown. The lower and upper boundaries of the box represent the 25% and 75% percentiles.

(B) Correlation between normalized CD177 values of gene expression measured by RNA-seq and CD177 protein by ELISA (ng/mL) from 36 patients with COVID-19. The blue line represents the linear regression line and the gray area the 95% prediction confidence interval.

(C) Association between CD177 serum concentration and time from symptom onset to the admission ($n = 192$). This association was tested using Spearman correlation tests. The blue line represents the linear regression line and the gray area the 95% confidence interval.

(D) Measurement of CD177 serum concentration in patients hospitalized in an intensive care unit (ICU) or not ($n = 196$). Wilcoxon rank tests were used. The median values (horizontal line in the boxplot) are shown. The lower and upper boundaries of the box represent the 25% and 75% percentiles.

(E) Change of CD177 concentration over time according to the occurrence of death for 172 patients with COVID-19 and a total of 248 measurements. Predictions were calculated using a mixed effect models for longitudinal data.

See also [Figure S6](#).

We then examined the dynamics of the CD177 concentration in 172 patients with COVID-19, with longitudinal serum samples, using all available measurements ([Figure 6E](#)). At the first measurement, the average concentration of CD177 was not significantly different between the patients who died and those who recovered (5.93 vs 5.06, $P = 0.26$, Wald test). When looking at the change of CD177 concentration over time, it appears clearly that the concentration was decreasing in those who recovered (-0.22 ng/mL/day, 95% CI -0.307 ; -0.139), whereas it was stable in those who died later on ($+0.10$ ng/mL/day, 95% confidence interval -0.014 ; $+0.192$). These results show that the stability of CD177 protein levels in patients with severe COVID-19 during the course of the disease is a hallmark of a worse prognosis, leading to death.

DISCUSSION

Here, we investigated factors that influence the clinical outcomes of patients with severe COVID-19 involved in a multicentric French cohort combining standardized whole-blood RNA-seq analyses, in-depth phenotypic analysis of immune cells, and measurements of a large panel of serum analytes. An integrated

and global overview of host markers revealed several pathways associated with the course of COVID-19 disease, with a prominent role for neutrophil activation. This signature included CD177, a specific neutrophil marker of activation, adhesion to the endothelium, and transmigration. The correlation between *CD177* gene abundance and serum protein levels in the blood of patients with COVID-19 underscores the importance of this marker, making the measurement of CD177 protein levels a reliable approach that is largely accessible in routine care. We also demonstrated that the dynamics of serum CD177 levels is strongly associated with the severity of COVID-19 disease, ICU hospitalization, and survival in an additional cohort of patients. During follow-up, the CD177 protein levels decrease in patients who are recovering, while staying high in those who died.

CD177 is a glycosylphosphatidylinositol (GPI)-anchored protein expressed by a variable proportion of human neutrophils. It plays a key role in the regulation of neutrophils by modulating their migration and activation. For example, the CD177 molecule has been identified as the most dysregulated parameter in purified neutrophils from patients with septic shock (Demaret et al., 2016) and in severe influenza (Tang et al., 2019). Clinically, neutrophil chemotaxis, infiltration of endothelial cells, and extravasation into alveolar spaces have been described in lung autopsies from deceased patients with COVID-19 (Fu et al., 2020). Elevated *CD177* mRNA expression has also been described for patients with acute Kawasaki disease (Huang et al., 2019) and resistant to IVIg therapy (Jing et al., 2020; Ko et al., 2019), a syndrome that has been described as a possible complication of SARS-CoV-2 infection in children (Toubiana et al., 2020; Viner and Whittaker, 2020). Our results are also consistent with those obtained using animal models, suggesting an important role for neutrophil activation in the severity of infection with respiratory viruses through their migration toward infected lungs, and in humans infected with influenza (Brandes et al., 2013; Narasaraju et al., 2011; Zaas et al., 2009).

The neutrophil activation signature is a specific feature of the homing of activated neutrophils toward infected lung tissue in acute lung injury (Juss et al., 2016), followed by the initiation of aggressive responses and the release of neutrophil extracellular traps (NETs), leading to an oxidative burst and the initiation of thrombus formation (Darbousset et al., 2012). Previous studies have reported elevated levels of circulating NETs in COVID-19 (Barnes et al., 2020a). Consistent with this finding and extending these data, we showed the differential expression of NET-related genes (Brandes et al., 2013; Narasaraju et al., 2011; Tang et al., 2019) (*S100A8*, *S100A9*, and *S100A12*), confirming the recently described elevated expression of calprotectin (heterodimer of *S100A8* and *A9*) in patients with severe COVID-19 (Silvin et al., 2020). The association of neutrophil activation signature with COVID-19 severity has also been described recently with *CD177* gene being one of the most differentially expressed gene in advanced disease (Aschenbrenner et al., 2021; Schulte-Schrepping et al., 2020). Likely, we believe that our data extended significantly these recent observations showing that CD177 is increased both at the level of coding RNA and at the protein level. Moreover, we show also that CD177 is not only a marker of severity but also of death as revealed by the longitudinal analysis which was confirmed in a second cohort.

Although, it is difficult to formally conclude whether CD177 is a causal factor of disease progression or a consequence of the severity of the disease, our data strongly show that CD177 is a valid hallmark of the physiopathology of COVID-19. This observation suggests that the activation of neutrophils, triggered by the infection, is a fundamental element of the innate response. However, persistent activation of this pathway may constitute, along with other factors (e.g., "cytokine storm"), fatal harm possibly associated with the critical turning point in the clinical trajectory of patients during the second week of the infection.

Neutrophil activation was associated with significant changes in the level of gene expression of several pathways, some concordantly associated with disturbances in immune-cell populations and cytokine and inflammatory profiles. We reveal a complex picture of the activation of innate immunity, assessed by significant changes in the expression of several genes involved in IFN signaling and the response to stress and the production of inflammatory/activation markers, with a balance between proinflammatory signals (increased expression of IL-1R1, IL-18R1, and its accessory chain IL-18 RAP) and anti-inflammatory cytokines or regulators (increased expression of IL-10, IL-4R, IL-27, IL-1RN) (Kim et al., 2005; Migliorini et al., 2020). The frequency of $\gamma\delta$ T cells, a subpopulation of CD3⁺ T cells that were first described in the lung (Augustin et al., 1989) and that play critical roles in anti-viral immune responses, tissue healing, and epithelial cell maintenance (Cheng and Hu, 2017), was elevated and they expressed an activation marker (CD16) and low levels of the inhibitory receptor NKG2A, suggesting possible killing capacity. In accordance with our observation that eIF2 signaling is significantly inhibited in patients with COVID-19, recent studies have shown that coronaviruses encode ISR antagonists, which act as competitive inhibitors of eIF2 signaling (Rabouw et al., 2016,

2020). Similarly, the inhibition of mTOR signaling that we found in patients with COVID-19 is consistent with the impaired mTOR signaling reported in blood myeloid dendritic cells of patients with COVID-19 (Arunachalam et al., 2020). Interestingly, we observed a markedly smaller proportion of all DC (pre-DC, pDC, cDC1, and cDC2) and monocyte cell populations, including classical, intermediate, and nonclassical subpopulations, in patients with COVID-19 than in HDs. Based on these observations, it can be hypothesized that the impairment in IFN- α production observed in patients with severe COVID-19 may be the result of both a decrease in the number of pDCs, which are natural IFN-producing cells (Ali et al., 2019), and inhibition of mTOR signaling, a regulator of IFN- α production, in these cells (Kaur et al., 2012).

We confirmed the previously reported expansion of B cell populations (Arunachalam et al., 2020; Bouadma et al., 2020) in patients with COVID-19, and our results showed that the anti-SARS-CoV-2 B cell repertoire is commonly mobilized. The marked upregulation of IGV gene families included the *IgHV1-24* family, described to be specific for COVID-19 (Brouwer et al., 2020). The expanded *VH4-39* family was also recently reported to be the most highly represented in S-specific SARS-CoV-2 sequences (Brouwer et al., 2020). We also found enrichment of *VH3-33*, previously described in a set of clonally related anti-SARS-CoV-2 receptor-binding domain antibodies (Barnes et al., 2020b).

Globally, these results show that the defense against SARS-CoV-2 after pathogen recognition triggers a fine-tuned program that not only includes the production of antiviral (IFN signaling) and proinflammatory cytokines but also signals the cessation of the response and a strong disturbance of adaptive immunity.

The same pathways (immune and stress responses through eIF2 signaling, neutrophil and IFN signaling, T and B cell receptor responses, and mTOR pathways) contributed to the ability to discriminate between three groups of patients with severe COVID-19 in an unsupervised analysis. One limitation of our study was that we did not repeat the RNA-seq analyses in these specific groups of patients. Nonetheless, it is noteworthy that these groups differed significantly by the time from disease onset. These findings provide clues in our understanding of the wide range of profiles previously described for COVID-19 by showing that these patterns may be mainly related to time-dependent changes in the blood during the course of the infection (Laing et al., 2020; Ong et al., 2020). For example, the observed lower abundance of IFN signaling genes in the last group of patients with COVID-19 may be owing to decreased abundance in more advanced disease and/or patients who constitutively present a lower abundance of ISG, as described in previous studies (Bastard et al., 2020).

Several months after the emergence of this new disease, treatment options for patients with severe disease requiring hospitalization are still limited to corticosteroids, which has emerged as the treatment of choice for critically ill patients (Prescott and Rice, 2020; Sterne et al., 2020). However, interventions that can be administered early during the course of infection to prevent disease progression and longer-term complications are urgently needed. A major obstacle for the design of “adapted” therapies to the various stages of disease evolution is a lack of markers associated with sudden worsening of the disease of patients with moderate to severe disease and markers to predict improvement. Our results show that the measurement of CD177 during the course of the disease may be helpful in following the response to treatment and revision of the prognosis. In addition, they suggest that therapies aiming to control neutrophil activation and chemotaxis should be considered for the treatment of hospitalized patients.

Limitations of the study

HDs were collected from the French Blood Donors Organization (Etablissement Français du sang) before the COVID-19 outbreak. Age to donate blood is limited between 18 and 65 years (with the necessary medical agreement beyond 60 years). Owing to the age of hospitalized patients with COVID-19 (median: 61 years), it was not possible to have age-matched HDs. So we could not exclude that differences observed between HD and patients with COVID-19 could be associated to the age difference. Samples were not available for the entire cohort of 61 patients for every experimentation but clinical characteristics were not different between included and excluded patients for each assay, that is cell phenotype (all $p > 0.97$), seric markers (all $p > 0.58$) and gene expression (all $p > 0.15$). Finally, although we have identified a set of gene characterizing activation of a neutrophil pathway in patients, as well as an association with increased serum CD177, a marker highly specific of neutrophils, we did not study the phenotype of blood neutrophils from patients included in our cohorts for practical reasons.

STAR★METHODS

Detailed methods are provided in the online version of this paper and include the following:

- **KEY RESOURCES TABLE**
- **RESOURCE AVAILABILITY**
 - Lead contact
 - Materials availability
 - Data and code availability
- **EXPERIMENTAL MODEL AND SUBJECT DETAILS**
 - Subjects
- **METHOD DETAILS**
 - Quantification of serum analytes
 - Cell phenotyping
 - RNA sequencing
- **QUANTIFICATION AND STATISTICAL ANALYSIS**
- **ADDITIONAL RESSOURCES**

SUPPLEMENTAL INFORMATION

Supplemental information can be found online at <https://doi.org/10.1016/j.isci.2021.102711>.

ACKNOWLEDGMENTS

We thank the patients who donated their blood. We thank F. Mentre, S. Tubiana, the French COVID cohort, and REACTing (REsearch & ACTION emergING infectious diseases) for cohort management. We thank the scientific advisory board of the French COVID-19 cohort composed of Dominique Costagliola, Astrid Vabret, Hervé Raoul, and Laurence Weiss. We thank Romain Lévy for fruitful discussions. This work was supported by INSERM and the Investissements d’Avenir program, Vaccine Research Institute (VRI), managed by the ANR under reference ANR-10-LABX-77-01 and the CARE project funded from the Innovative Medicines Initiative 2 Joint Undertaking (JU) under grant agreement No 101005077. The JU receives support from the European Union’s Horizon 2020 research and innovation programme and EFPIA and Bill & Melinda Gates Foundation, Global Health Drug Discovery Institute, University of Dundee. The French COVID Cohort is funded through the Ministry of Health and Social Affairs and Ministry of Higher Education and Research dedicated COVID19 fund and PHRC n°20-0424 and the REACTing consortium. Funding sources were not involved in the study design, data acquisition, data analysis, data interpretation, or writing of the manuscript.

AUTHOR CONTRIBUTIONS

YL and AW conceived and designed the study. MC, JFT, YY, LB, DB, CLa, GP, and MP participated in sample and clinical data collection. EF, MDe, MS, CLe, and PT performed the experiments. MD, MG, BH, and CLe analyzed the data. YL, RT, AW, HH, MS, BJH, and CL analyzed and interpreted the data. YL, RT, AW, and HH drafted the first version and wrote the final version of the manuscript. All authors approved the final version.

DECLARATION OF INTERESTS

None of the authors has any conflict of interest to declare.

Received: February 8, 2021

Revised: March 26, 2021

Accepted: June 8, 2021

Published: July 23, 2021

REFERENCES

- Ali, S., Mann-Nüttel, R., Schulze, A., Richter, L., Alferink, J., and Scheu, S. (2019). Sources of type I interferons in infectious immunity: plasmacytoid dendritic cells not always in the driver’s seat. *Front. Immunol.* 10, 778.
- Argelaguet, R., Clark, S.J., Mohammed, H., Stapel, L.C., Krueger, C., Kapourani, C.A., Imaz-Rosshandler, I., Lohoff, T., Xiang, Y.L., Hanna, C.W., et al. (2019). Multi-omics profiling of mouse gastrulation at single-cell resolution. *Nature* 576, 487.
- Arunachalam, P.S., Wimmers, F., Mok, C.K.P., Perera, R., Scott, M., Hagan, T., Sigal, N., Feng, Y., Bristow, L., Tak-Yin Tsang, O., et al. (2020). Systems biological assessment of immunity to mild versus severe

COVID-19 infection in humans. *Science* 369, 1210–1220.

Aschenbrenner, A.C., Moukhtaroudi, M., Krämer, B., Oestreich, M., Antonakos, N., Nuesch-Germano, M., Gkizeli, K., Bonaguro, L., Reusch, N., Baßler, K., et al. (2021). Disease severity-specific neutrophil signatures in blood transcriptomes stratify COVID-19 patients. *Genome Med.* 13, 7.

Augustin, A., Kubo, R.T., and Sim, G.K. (1989). Resident pulmonary lymphocytes expressing the gamma/delta T-cell receptor. *Nature* 340, 239–241.

Barnes, B.J., Adrover, J.M., Baxter-Stoltzfus, A., Borczuk, A., Cools-Lartigue, J., Crawford, J.M., Daßler-Plenker, J., Guerci, P., Huynh, C., Knight, J.S., et al. (2020a). Targeting potential drivers of COVID-19: neutrophil extracellular traps. *J. Exp. Med.* 217, e20200652.

Barnes, C.O., West, A.P., Jr., Huey-Tubman, K.E., Hoffmann, M.A.G., Sharaf, N.G., Hoffman, P.R., Koranda, N., Gristick, H.B., Gaebler, C., Muecksch, F., et al. (2020b). Structures of human antibodies bound to SARS-CoV-2 spike reveal common epitopes and recurrent features of antibodies. *Cell* 182, 828–842 e816.

Bastard, P., Rosen, L.B., Zhang, Q., Michailidis, E., Hoffmann, H.-H., Zhang, Y., Dorgham, K., Philippot, Q., Rosain, J., Béziat, V., et al. (2020). Autoantibodies against type I IFNs in patients with life-threatening COVID-19. *Science* 370, eabd4585.

Bayat, B., Werth, S., Sachs, U.J.H., Newman, D.K., Newman, P.J., and Santoso, S. (2010). Neutrophil transmigration mediated by the neutrophil-specific antigen CD177 is influenced by the endothelial S536N dimorphism of platelet endothelial cell adhesion molecule-1. *J. Immunol.* 184, 3889–3896.

Blanco-Melo, D., Nilsson-Payant, B.E., Liu, W.C., Uhl, S., Hoagland, D., Moller, R., Jordan, T.X., Oishi, K., Panis, M., Sachs, D., et al. (2020). Imbalanced host response to SARS-CoV-2 drives development of COVID-19. *Cell* 181, 1036–1045 e1039.

Bouadma, L., Wiedemann, A., Patrier, J., Surenaud, M., Wicky, P.H., Foucat, E., Diehl, J.L., Hejblum, B.P., Sinnah, F., de Montmollin, E., et al. (2020). Immune alterations in a patient with SARS-CoV-2-related acute respiratory distress syndrome. *J. Clin. Immunol.* 40, 1082–1092.

Boyd, J.H., Fjell, C.D., Russell, J.A., Sirounis, D., Cirstea, M.S., and Walley, K.R. (2016). Increased plasma PCSK9 levels are associated with reduced endotoxin clearance and the development of acute organ failures during sepsis. *J. Innate Immun.* 8, 211–220.

Brandes, M., Klauschen, F., Kuchen, S., and Germain, R.N. (2013). A systems analysis identifies a feedforward inflammatory circuit leading to lethal influenza infection. *Cell* 154, 197–212.

Brouwer, P.J.M., Caniels, T.G., van der Straten, K., Snitselaar, J.L., Aldon, Y., Bangaru, S., Torres, J.L., Okba, N.M.A., Claireaux, M., Kerster, G., et al. (2020). Potent neutralizing antibodies from COVID-19 patients define multiple targets of vulnerability. *Science* 369, 643–650.

Buechler, C., Eisinger, K., and Krautbauer, S. (2013). Diagnostic and prognostic potential of the

macrophage specific receptor CD163 in inflammatory diseases. *Inflamm. Allergy Drug Targets* 12, 391–402.

Cai, Y.Q., Lv, Y., Mo, Z.C., Lei, J., Zhu, J.L., and Zhong, Q.Q. (2020). Multiple pathophysiological roles of midkine in human disease. *Cytokine* 135, 155242.

Chen, G., Wu, D., Guo, W., Cao, Y., Huang, D., Wang, H., Wang, T., Zhang, X., Chen, H., Yu, H., et al. (2020a). Clinical and immunological features of severe and moderate coronavirus disease 2019. *J. Clin. Invest.* 130, 2620–2629.

Chen, N., Zhou, M., Dong, X., Qu, J., Gong, F., Han, Y., Qiu, Y., Wang, J., Liu, Y., Wei, Y., et al. (2020b). Epidemiological and clinical characteristics of 99 cases of 2019 novel coronavirus pneumonia in Wuhan, China: a descriptive study. *Lancet* 395, 507–513.

Cheng, M., and Hu, S. (2017). Lung-resident gammadelta T cells and their roles in lung diseases. *Immunology* 151, 375–384.

Coronaviridae Study Group of the International Committee on Taxonomy of V. (2020). The species Severe acute respiratory syndrome-related coronavirus: classifying 2019-nCoV and naming it SARS-CoV-2. *Nat. Microbiol.* 5, 536–544.

Darbousset, R., Thomas, G.M., Mezouar, S., Frère, C., Bonier, R., Mackman, N., Renné, T., Dignat-George, F., Dubois, C., and Panicot-Dubois, L. (2012). Tissue factor-positive neutrophils bind to injured endothelial wall and initiate thrombus formation. *Blood* 120, 2133–2143.

De Biasi, S., Meschieri, M., Gibellini, L., Bellinazzi, C., Borella, R., Fidanza, L., Gozzi, L., Iannone, A., Lo Tartaro, D., Mattioli, M., et al. (2020). Marked T cell activation, senescence, exhaustion and skewing towards TH17 in patients with COVID-19 pneumonia. *Nat. Commun.* 11, 3434.

Demaret, J., Venet, F., Plassais, J., Cazalis, M.-A., Vallin, H., Friggeri, A., Lepape, A., Rimmelé, T., Textoris, J., and Monneret, G. (2016). Identification of CD177 as the most dysregulated parameter in a microarray study of purified neutrophils from septic shock patients. *Immunol. Lett.* 178, 122–130.

Durinck, S., Spellman, P.T., Birney, E., and Huber, W. (2009). Mapping identifiers for the integration of genomic datasets with the R/Bioconductor package biomaRt. *Nat. Protoc.* 4, 1184–1191.

Dwivedi, D.J., Grin, P.M., Khan, M., Prat, A., Zhou, J., Fox-Robichaud, A.E., Seidah, N.G., and Liaw, P.C. (2016). Differential expression of PCSK9 modulates infection, inflammation, and coagulation in a murine model of sepsis. *Shock* 46, 672–680.

Fu, J., Kong, J., Wang, W., Wu, M., Yao, L., Wang, Z., Jin, J., Wu, D., and Yu, X. (2020). The clinical implication of dynamic neutrophil to lymphocyte ratio and D-dimer in COVID-19: a retrospective study in Suzhou China. *Thromb. Res.* 192, 3–8.

Gan, E.S., Tan, H.C., Duyen, H.L.T., Trieu, H.T., Wills, B., Ooi, E.E., Seidah, N.G., and Yacoub, S. (2020). Dengue virus induces PCSK9 expression to alter antiviral responses and disease outcomes. *J. Clin. Invest.* 130, 5223–5234.

Gauthier, M., Agniel, D., Thiébaud, R., and Hejblum, B.P. (2019). dearseq: a variance component score test for RNA-Seq differential analysis that effectively controls the false discovery rate. *NAR Genom. Bioinform.* 2, lqaa093.

Giamarellos-Bourboulis, E.J., Netea, M.G., Rovina, N., Akinosoglou, K., Antoniadou, A., Antonakos, N., Damoraki, G., Gkavogianni, T., Adami, M.E., Katsaounou, P., et al. (2020). Complex immune dysregulation in COVID-19 patients with severe respiratory failure. *Cell Host Microbe* 27, 992–1000 e1003.

Hadjadji, J., Yatim, N., Barnabei, L., Corneau, A., Boussier, J., Smith, N., Pere, H., Charbit, B., Bondet, V., Chenevier-Gobeaux, C., et al. (2020). Impaired type I interferon activity and inflammatory responses in severe COVID-19 patients. *Science* 369, 718–724.

Huang, C., Wang, Y., Li, X., Ren, L., Zhao, J., Hu, Y., Zhang, L., Fan, G., Xu, J., Gu, X., et al. (2020). Clinical features of patients infected with 2019 novel coronavirus in Wuhan, China. *Lancet* 395, 497–506.

Huang, W.D., Lin, Y.T., Tsai, Z.Y., Chang, L.S., Liu, S.F., Lin, Y.J., and Kuo, H.C. (2019). Association between maternal age and outcomes in Kawasaki disease patients. *Pediatr. Rheumatol.* 17, 46.

Jing, Y., Ding, M., Fu, J., Xiao, Y., Chen, X., and Zhang, Q. (2020). Neutrophil extracellular trap from Kawasaki disease alter the biologic responses of PBMC. *Biosci. Rep.* 40, BSR20200928.

Juss, J.K., House, D., Amour, A., Begg, M., Herre, J., Storisteanu, D.M.L., Hoenderdos, K., Bradley, G., Lennon, M., Summers, C., et al. (2016). Acute respiratory distress syndrome neutrophils have a distinct phenotype and are resistant to phosphoinositide 3-kinase inhibition. *Am. J. Resp. Crit. Care* 194, 961–973.

Kaur, S., Sassano, A., Majchrzak-Kita, B., Baker, D.P., Su, B., Fish, E.N., and Platanias, L.C. (2012). Regulatory effects of mTORC2 complexes in type I IFN signaling and in the generation of IFN responses. *Proc. Natl. Acad. Sci.* 109, 7723–7728.

Kim, S.H., Han, S.Y., Azam, T., Yoon, D.Y., and Dinarello, C.A. (2005). Interleukin-32: a cytokine and inducer of TNFalpha. *Immunity* 22, 131–142.

Ko, T.M., Chang, J.S., Chen, S.P., Liu, Y.M., Chang, C.J., Tsai, F.J., Lee, Y.C., Chen, C.H., Chen, Y.T., and Wu, J.Y. (2019). Genome-wide transcriptome analysis to further understand neutrophil activation and lncRNA transcript profiles in Kawasaki disease. *Sci. Rep.* 9, 328.

Kuri-Cervantes, L., Pampena, M.B., Meng, W., Rosenfeld, A.M., Ittner, C.A.G., Weisman, A.R., Agyekum, R., Mathew, D., Baxter, A.E., Vella, L., et al. (2020). Immunologic Perturbations in Severe COVID-19/sars-CoV-2 Infection (bioRxiv).

Laing, A.G., Lorenc, A., Del Molino Del Barrio, I., Das, A., Fish, M., Monin, L., Munoz-Ruiz, M., McKenzie, D.R., Hayday, T.S., Francos-Quijorna, I., et al. (2020). A dynamic COVID-19 immune signature includes associations with poor prognosis. *Nat. Med.* 26, 1623–1635.

Le Gall, J.R. (1993). A new Simplified Acute Physiology Score (SAPS II) based on a European/

- North American multicenter study. *JAMA* 270, 2957–2963.
- Levin, D., and London, I.M. (1978). Regulation of protein synthesis: activation by double-stranded RNA of a protein kinase that phosphorylates eukaryotic initiation factor 2. *Proc. Natl. Acad. Sci. U S A* 75, 1121–1125.
- Lucas, C., Wong, P., Klein, J., Castro, T.B.R., Silva, J., Sundaram, M., Ellingson, M.K., Mao, T., Oh, J.E., Israelow, B., et al. (2020). Longitudinal analyses reveal immunological misfiring in severe COVID-19. *Nature* 584, 463–469.
- Mathew, D., Giles, J.R., Baxter, A.E., Oldridge, D.A., Greenplate, A.R., Wu, J.E., Alanio, C., Kuri-Cervantes, L., Pampena, M.B., D'Andrea, K., et al. (2020). Deep immune profiling of COVID-19 patients reveals distinct immunotypes with therapeutic implications. *Science* 369, eabc8511.
- Mehta, P., McAuley, D.F., Brown, M., Sanchez, E., Tattersall, R.S., and Manson, J.J. (2020). COVID-19: consider cytokine storm syndromes and immunosuppression. *Lancet* 395, 1033–1034.
- Migliorini, P., Italiani, P., Pratesi, F., Puxeddu, I., and Boraschi, D. (2020). The IL-1 family cytokines and receptors in autoimmune diseases. *Autoimmun. Rev.* 19, 102617.
- Narasaraju, T., Yang, E., Samy, R.P., Ng, H.H., Poh, W.P., Liew, A.A., Phoon, M.C., van Rooijen, N., and Chow, V.T. (2011). Excessive neutrophils and neutrophil extracellular traps contribute to acute lung injury of influenza pneumonitis. *Am. J. Pathol.* 179, 199–210.
- Ong, E.Z., Chan, Y.F.Z., Leong, W.Y., Lee, N.M.Y., Kalimuddin, S., Haja Mohideen, S.M., Chan, K.S., Tan, A.T., Bertolotti, A., Ooi, E.E., et al. (2020). A dynamic immune response shapes COVID-19 progression. *Cell Host Microbe* 27, 879–882 e872.
- Pakos-Zebrucka, K., Koryga, I., Mnich, K., Ljujic, M., Samali, A., and Gorman, A.M. (2016). The integrated stress response. *EMBO Rep.* 17, 1374–1395.
- Patro, R., Duggal, G., Love, M.I., Irizarry, R.A., and Kingsford, C. (2017). Salmon provides fast and bias-aware quantification of transcript expression. *Nat. Methods* 14, 417–419.
- Phelan, A.L., Katz, R., and Gostin, L.O. (2020). The novel coronavirus originating in wuhan, China: challenges for global health governance. *JAMA* 323, 709–710.
- Ponti, G., Maccaferri, M., Ruini, C., Tomasi, A., and Ozben, T. (2020). Biomarkers associated with COVID-19 disease progression. *Crit. Rev. Clin. Lab. Sci.* 57, 389–399.
- Prescott, H.C., and Rice, T.W. (2020). Corticosteroids in COVID-19 ARDS. *JAMA* 324, 1292.
- Qin, C., Zhou, L., Hu, Z., Zhang, S., Yang, S., Tao, Y., Xie, C., Ma, K., Shang, K., Wang, W., et al. (2020). Dysregulation of immune response in patients with COVID-19 in Wuhan, China. *Clin. Infect. Dis.* 71, 762–768.
- Rabouw, H.H., Langereis, M.A., Knaap, R.C., Dalebout, T.J., Canton, J., Sola, I., Enjuanes, L., Bredenoord, P.J., Kikkert, M., de Groot, R.J., et al. (2016). Middle East respiratory coronavirus accessory protein 4a inhibits PKR-mediated antiviral stress responses. *PLoS Pathog.* 12, e1005982.
- Rabouw, H.H., Visser, L.J., Passchier, T.C., Langereis, M.A., Liu, F., Giansanti, P., van Vliet, A.L.W., Dekker, J.G., van der Grein, S.G., Saucedo, J.G., et al. (2020). Inhibition of the integrated stress response by viral proteins that block p-eIF2-eIF2B association. *Nat. Microbiol.* 5, 1361–1373.
- Roth, J., Vogl, T., Sorg, C., and Sunderkötter, C. (2003). Phagocyte-specific S100 proteins: a novel group of proinflammatory molecules. *Trends Immunol.* 24, 155–158.
- Schulte-Schrepping, J., Reusch, N., Paclik, D., Baßler, K., Schlickeiser, S., Zhang, B., Krämer, B., Krammer, T., Brumhard, S., Bonaguro, L., et al. (2020). Severe COVID-19 is marked by a dysregulated myeloid cell compartment. *Cell* 182, 1419–1440.e1423.
- See, P., Dutertre, C.A., Chen, J., Gunther, P., McGovern, N., Irac, S.E., Gunawan, M., Beyer, M., Handler, K., Duan, K., et al. (2017). Mapping the human DC lineage through the integration of high-dimensional techniques. *Science* 356, eaag3009.
- Shen-Orr, S.S., Tibshirani, R., Khatri, P., Bodian, D.L., Staedtler, F., Perry, N.M., Hastie, T., Sarwal, M.M., Davis, M.M., and Butte, A.J. (2010). Cell type-specific gene expression differences in complex tissues. *Nat. Methods* 7, 287–289.
- Silvin, A., Chapuis, N., Dunsmore, G., Goubet, A.G., Dubuisson, A., Derosa, L., Almiré, C., Henon, C., Kosmider, O., Droin, N., et al. (2020). Elevated Calprotectin and abnormal myeloid cell subsets discriminate severe from mild COVID-19. *Cell* 182, 1401–1418.e18.
- Sterne, J.A.C., Murthy, S., Diaz, J.V., Slutsky, A.S., Villar, J., Angus, D.C., Annane, D., Azevedo, L.C.P., Berwanger, O., Cavalcanti, A.B., et al. (2020). Association between administration of systemic corticosteroids and mortality among critically ill patients with COVID-19. *JAMA* 324, 1330.
- Tang, B.M., Shojaei, M., Teoh, S., Meyers, A., Ho, J., Ball, T.B., Keynan, Y., Pisipati, A., Kumar, A., Eisen, D.P., et al. (2019). Neutrophils-related host factors associated with severe disease and fatality in patients with influenza infection. *Nat. Commun.* 10, 3422.
- Theilgaard-Monch, K. (2006). Haptoglobin is synthesized during granulocyte differentiation, stored in specific granules, and released by neutrophils in response to activation. *Blood* 108, 353–361.
- Toubiana, J., Poirault, C., Corsia, A., Bajolle, F., Fourgeaud, J., Angoulvant, F., Debray, A., Basmaci, R., Salvador, E., Biscardi, S., et al. (2020). Kawasaki-like multisystem inflammatory syndrome in children during the covid-19 pandemic in Paris, France: prospective observational study. *BMJ* 369, m2094.
- Vincent, J.-L., de Mendonca, A., Cantraine, F., Moreno, R., Takala, J., Suter, P.M., Sprung, C.L., Colardyn, F., and Blecher, S. (1998). Use of the SOFA score to assess the incidence of organ dysfunction/failure in intensive care units. *Crit. Care Med.* 26, 1793–1800.
- Viner, R.M., and Whittaker, E. (2020). Kawasaki-like disease: emerging complication during the COVID-19 pandemic. *Lancet* 395, 1741–1743.
- Wilk, A.J., Rustagi, A., Zhao, N.Q., Roque, J., Martinez-Colon, G.J., McKechnie, J.L., Iverson, G.T., Ranganath, T., Vergara, R., Hollis, T., et al. (2020). A single-cell atlas of the peripheral immune response in patients with severe COVID-19. *Nat. Med.* 26, 1070–1076.
- Wu, Z.Y., and McGoogan, J.M. (2020). Characteristics of and important lessons from the coronavirus disease 2019 (COVID-19) outbreak in China summary of a report of 72 314 cases from the Chinese center for disease control and prevention. *JAMA* 323, 1239–1242.
- Xu, B., Fan, C.Y., Wang, A.L., Zou, Y.L., Yu, Y.H., He, C., Xia, W.G., Zhang, J.X., and Miao, Q. (2020). Suppressed T cell-mediated immunity in patients with COVID-19: a clinical retrospective study in Wuhan, China. *J. Infect.* 81, e51–e60.
- Yazdanpanah, Y. (2020). Impact on disease mortality of clinical, biological, and virological characteristics at hospital admission and overtime in COVID-19 patients. *J. Med. Virol.* 93, 2149–2159.
- Zaas, A.K., Chen, M., Varkey, J., Veldman, T., Hero, A.O., Lucas, J., Huang, Y., Turner, R., Gilbert, A., Lambkin-Williams, R., et al. (2009). Gene expression signatures diagnose influenza and other symptomatic respiratory viral infections in humans. *Cell Host Microbe* 6, 207–217.
- Zhi, Y., Gao, P., Xin, X., Li, W., Ji, L., Zhang, L., Zhang, X., and Zhang, J. (2017). Clinical significance of sCD163 and its possible role in asthma (Review). *Mol. Med. Rep.* 15, 2931–2939.
- Zhou, Z., Ren, L., Zhang, L., Zhong, J., Xiao, Y., Jia, Z., Guo, L., Yang, J., Wang, C., Jiang, S., et al. (2020). Heightened innate immune responses in the respiratory tract of COVID-19 patients. *Cell Host Microbe* 27, 883–890 e882.

STAR★METHODS

KEY RESOURCES TABLE

REAGENT or RESOURCE	SOURCE	IDENTIFIER
Antibodies		
Mouse Monoclonal anti-CD38 FITC	BD Biosciences	#340909
Mouse Monoclonal anti-HLADR PE	BD Biosciences	#347401
Mouse Monoclonal anti-CD4 BV421	BD Biosciences	#562424
Mouse Monoclonal anti-CD8 APCH7	BD Biosciences	#560179
Mouse Monoclonal anti-CD3 Alexa 700	BD Biosciences	#557943
Rat Monoclonal anti-CCR7 Alexa647	BD Biosciences	#557734
Mouse Monoclonal anti-CD21 PE	BD Biosciences	#555422
Mouse Monoclonal anti-CD27 APC	BD Biosciences	#337169
Mouse Monoclonal anti-CD45 Alexa 700	BD Biosciences	#560566
Mouse Monoclonal anti-CD56 PECF594	BD Biosciences	#564849
Mouse Monoclonal anti-HLADR BV605	BD Biosciences	#562845
Mouse Monoclonal anti-CD33 BV421	BD Biosciences	#562854
Mouse Monoclonal anti-CD141 BV711	BD Biosciences	#563155
Mouse Monoclonal anti-CD45RA PerCpCy5.5	BD Biosciences	#563429
Mouse Monoclonal anti-HLA ABC BV786	BD Biosciences	#740982
Mouse Monoclonal anti-CD86 PECF594	BD Biosciences	#562390
Mouse Monoclonal anti-PD1 BV605	BD Biosciences	#563245
Mouse Monoclonal anti-TCR gamma delta	BD Biosciences	#559878
Mouse Monoclonal anti-CD45RA PEfluor 610	ebiosciences	#61-0458-42
Mouse Monoclonal anti-Ki67 PercPe710	ebiosciences	#46-5698-82
Mouse Monoclonal anti-CD19 PC7	Beckman Coulter	#IM3628
Mouse Monoclonal anti-CD38 PercpCy5.5	Biolegend	#303522
Mouse Monoclonal anti-IgM Pacific Blue	Biolegend	#314514
Mouse Monoclonal anti-CD16 APC Cy7	Biolegend	#302018
Mouse Monoclonal anti-CD14 BV605	Biolegend	#301834
Mouse Monoclonal anti-CD1c PECy7	Biolegend	#331516
Mouse Monoclonal anti-CD40 PE	Biolegend	#334308
Mouse Monoclonal Lineage FITC	Biolegend	#348801
Mouse Monoclonal anti-CD57 PercPCy5.5	Biolegend	#359622
F(ab') ₂ -Goat anti-Human IgD FITC	Invitrogen	#H15501
Mouse Monoclonal anti-CD123 APC	Miltenyi Biotec	#130-113-322
Mouse Monoclonal anti-NKG2A PEVio770	Miltenyi Biotec	#130-113-567
BD Cytotfix/cytoperm fixation/permeabilization kit	BD Biosciences	# 554714
Biological Samples		
French COVID-19 patients	French COVID cohort	clinicaltrials.gov NCT04262921
Swiss COVID-19 patients	Swiss cohort	Swiss ethics protocol ID: 2020-00620
Critical Commercial Assays		
Human Magnetic Luminex Assay (CD163, ST2, and CD14, LBP)	R&D Systems	LXSAHM-2 kits
Human XL Cyt Disc Premixed Mag Luminex Perf Assay Kit	R&D Systems	LXSAHM-19 kit

(Continued on next page)

Continued

REAGENT or RESOURCE	SOURCE	IDENTIFIER
48-Plex Bio-Plex Pro Human Cytokine	Bio-Rad	#12007283
CD177 ELISA Kit	ThermoFisher Scientific	EH80RBX5

Deposited Data

Raw and analyzed data	This paper	GEO code: GSE171110
-----------------------	------------	---------------------

Software and Algorithms

DIVA v6.2	BD Biosciences	https://www.bdbiosciences.com/en-us/instruments/research-instruments/research-software/flow-cytometry-acquisition/facsdiva-software
Bio-Plex Manager v6.1	Biorad	https://www.bio-rad.com/fr-fr/product/bio-plex-manager-software-standard-edition?ID=5846e84e-03a7-4599-a8ae-7ba5dd2c7684
hg19 human reference genome	This paper	https://www.ncbi.nlm.nih.gov/assembly/GCF_000001405.13/
STAR - v. 2.5.3ar, and quantified relative to annotation model hg19 - GENCODE Genes - release 19	N/A	[https://www.genecodegenes.org/human/release_19.html]
Sequence Analysis Viewer (SAV) version 2.1.8.		
R (version 3.6)	The R Foundation for Statistical Computing, Vienna, Austria	https://www.r-project.org/
FlowJo v9	Treestar	https://www.flowjo.com/solutions/flowjo/downloads
SPICE v5.22	https://doi.org/10.1002/cyto.a.21015	(http://exon.niaid.nih.gov/spice)
Ingenuity Pathway software v.51963813.	Qiagen	Ingenuity Pathway Analysis (IPA) - QIAGEN Online Shop

RESOURCE AVAILABILITY

Lead contact

Further information and requests for resources should be directed to and will be fulfilled by the lead contact, Yves Lévy (yves.levy@aphp.fr).

Materials availability

No materials were newly generated for this paper.

Data and code availability

RNA sequencing data that support the findings of this study have been deposited in Gene Expression Omnibus repository with the accession codes GSE171110. Further information and requests for resources and reagents should be directed to and will be fulfilled by the lead contact: Yves Lévy (yves.levy@aphp.fr).

EXPERIMENTAL MODEL AND SUBJECT DETAILS

Subjects

We enrolled a subgroup of patients with COVID-19 of the prospective French COVID cohort in this immunological study which is part of the cohort main objectives. The median age of patients with COVID-19 was 60 years [50–69], and 80% were men. Ethics approval was given on February 5 by the French Ethics Committee CPP-Ile-de-France VI (ID RCB: 2020-A00256-33). Eligible patients were those who were hospitalized with virologically confirmed COVID-19. Briefly, nasopharyngeal swabs were performed on the day of inclusion for SARS-CoV-2 testing as per the World Health Organization (WHO) or French National Health Agency guidelines. Viral loads were quantified by real-time semiquantitative reverse transcriptase polymerase chain reactions using either the Charité WHO protocol (testing the E gene and RdRp) or the Pasteur

institute assay (testing the E gene and two other RdRp targets, IP2 and IP4). The study was conducted with the understanding and the consent of each participant or its surrogate covering the sampling, storage, and use of biological samples. The time from symptom onset to the admission has been retrospectively collected by the interview of patients enrolled in the national "French COVID-19 cohort." The Swiss cohort was approved by the ethical commission (CER-VD; Swiss ethics protocol ID: 2020-00620) and all subjects provided written informed consent. Blood from healthy donors (HDs) was collected from the French Blood Donors Organization (Etablissement Français du sang) before the COVID-19 outbreak. HD characteristics are shown in [Table S3](#).

METHOD DETAILS

Quantification of serum analytes

In total, 71 analytes were quantified in heat-inactivated serum samples by multiplex magnetic bead assays or ELISA. Serum samples from five healthy donors were also assayed as controls. The following kits were used as per the manufacturers' recommendations: LXSAHM-2 kits for CD163, ST2, CD14 and LBP (R&D Systems); the LXSAHM-19 kit for IL-21, IL-23, IL-31, EGF, Flt-3 Ligand, Granzyme B, Granzyme A, IL-25, PD-L1/B7-H1, TGF- α , Aggrecan, 4-1BB/CD137, Fas, FasL, CCL-28, Chemerin, sCD40L, CXCL14, and Midkine (R&D Systems); and the 48-Plex Bio-Plex Pro Human Cytokine screening kit for IL-1 β , IL-1 α , IL-2, IL-4, IL-5, IL-6, IL-7, IL-8 / CXCL8, IL-9, IL-10, IL-12 (p70), IL-13, IL-15, IL-17A / CTLA8, Basic FGF (FGF-2), Eotaxin / CCL11, G-CSF, GM-CSF, IFN- γ , IP-10/CXCL10, MCP-1 / CCL2, MIP-1 α / CCL3, MIP-1 β / CCL4, PDGF-BB (PDGF-AB/BB), RANTES/CCL5, TNF- α , VEGF (VEGF-A), IL-1a, IL-2Ra (IL-2R), IL-3, IL-12 (p40), IL-16, IL-18, CTACK / CCL27, GRO-a / CXCL1 (GRO), HGF, IFN- α 2, LIF, MCP-3 / CCL7, M-CSF, MIF, MIG/CXCL9, b-NGF, SCF, SCGF-b, SDF-1 α , TNF-b/LTA, and TRAIL (Bio-Rad). The data were acquired using a Bio-Plex 200 system. Extrapolated concentrations were used and the out-of-range values were entered at the highest or lowest extrapolated concentration. Values were standardized for each cytokine across all displayed samples (centered around the observed mean, with variance equal to 1). CD177 quantification was performed on non-inactivated serum samples (diluted 1:2 or 1:10) using a Human CD177 ELISA Kit (ThermoFisher Scientific), according to the manufacturer's instructions.

Cell phenotyping

Immune-cell phenotyping was performed using an LSR Fortessa 4-laser (488, 640, 561, and 405 nm) flow cytometer (BD Biosciences) and Diva software, version 6.2. FlowJo software, version 9.9.6 (Tree Star Inc.), was used for data analysis. CD4+ and CD8+ T cells were analyzed for CD45RA and CCR7 expression to identify the naive, memory, and effector cell subsets for coexpression of activation (HLA-DR and CD38) and exhaustion/senescence (CD57 and PD1) markers. CD19+ B cell subsets were analyzed for the markers CD21 and CD27. ASC (plasmablasts) were identified as CD19+ cells expressing CD38 and CD27. We used CD16, CD56, and CD57 to identify NK cell subsets. $\gamma\delta$ T cells were identified using an anti-TCR $\gamma\delta$ antibody. HLA-DR, CD33, CD45RA, CD123, CD141, and CD1c were used to identify dendritic cell subsets, as previously described ([See et al., 2017](#)). Extracellular labeling was performed for all antibodies except for Ki 67 for which an intracellular labeling was performed with the BD cytofix/cytoperm kit (BD Biosciences).

RNA sequencing

Total RNA was purified from whole blood using the Tempus™ Spin RNA Isolation Kit (ThermoFisher Scientific). RNA was quantified using the Quant-iT RiboGreen RNA Assay Kit (Thermo Fisher Scientific) and quality control performed on a Bioanalyzer (Agilent). Globin mRNA was depleted using GLOBINclear Kit (Invitrogen) before mRNA library preparation with the TruSeq® Stranded mRNA Kit, as per the Illumina protocol. Libraries were sequenced on an Illumina HiSeq 2500 V4 system. Sequencing quality control was performed using Sequence Analysis Viewer. FastQ files were generated on the Illumina BaseSpace Sequence Hub. Transcript reads were aligned to the hg18 human reference genome using Salmon v0.8.2 ([Patro et al., 2017](#)) and quantified relative to annotation model "hsapiens_gene_ensembl" recovered from the R package biomaRt v2.42.1 ([Durinck et al., 2009](#)). Quality control of the alignment was performed via MultiQC v1.4 ([Patro et al., 2017](#)). Finally, counts were normalized as counts per million.

QUANTIFICATION AND STATISTICAL ANALYSIS

Subgroups of patients with COVID-19 were identified from unsupervised hierarchical clustering of log2-counts-per-million RNA-seq transcriptomics from whole blood using the Euclidean distance and Ward's method. Differential expression analysis was carried out using dearseq ([Gauthier et al., 2019](#)) to contribute

to the analysis of genes of which the abundance differed across the three subgroups of patient with COVID-19 and healthy subjects. Once the groups were defined by hierarchical clustering, the analysis of the genes contributing to each group was performed by selecting genes with an absolute fold change of ≥ 1.5 in the comparison of interest for which the difference in expression between HDs and patients with COVID-19 was significant ($P \leq 0.05$) (to avoid so called “double dipping” [<https://arxiv.org/abs/2012.02936>]). Pathway analyses of the genes involved in each comparison was performed using Ingenuity Pathway Analysis (IPA®, Qiagen, Redwood City, California, Version 57662101, 2020). For canonical pathway analysis, a Z-score ≥ 2 was defined as the threshold for significant activation, whereas a Z-score ≤ -2 was defined as the threshold for significant inhibition.

The integrative analysis of the three types of biological data (RNA-seq, cell phenotypes, serum analytes) was performed using MOFA+ (Argelaguet et al., 2019), a sparse factor analysis method. It provides latent variables which are linear combination of the most influential factors for explaining interpatient variability across the three biological measurement modalities. The first component is presented and called integrative score here. The analyses of factors associated with CD177 protein concentration were performed using nonparametric Wilcoxon test or Spearman correlation coefficient when appropriate. To look at the independent association of CD177 with ICU, a logistic regression for the prediction of hospitalization in the ICU adjusted for age, sex, chronic cardiac disease, chronic pulmonary disease, and diabetes was fitted. The analysis of repeated measurements of CD177 over time was performed by using a linear mixed effect model adjusted for time from hospitalization and an interaction with survival outcome (death or recovery). The model included a random intercept and a random slope with an unstructured matrix for variance parameters. Predictions of marginal trajectories were performed. All analyses, if not stated otherwise, were performed using R software, version 3.6.3. R: A language and environment for statistical computing. R Foundation for Statistical Computing, Vienna, Austria. URL: <https://www.R-project.org/>

ADDITIONAL RESSOURCES

A subgroup of patients with COVID-19 of the prospective French COVID cohort was enrolled in this study. French COVID cohort was registered at: <https://clinicaltrials.gov/ct2/show/NCT04262921>